INRIA

INSTITUT NATIONAL DE RECHERCHE EN INFORMATIQUE ET EN AUTOMATIQUE

An Analysis of Higher Order Boundary Conditions for the Wave Equation.

Julien Diaz — Patrick Joly

N° 4962

Octobre 2003

THÈME 4

ISSN 0249-6399 ISRN INRIA/RR--4962--FR+ENG

INRIA
ROCQUENCOURT

An Analysis of Higher Order Boundary Conditions for the Wave Equation.

Julien Diaz , Patrick Joly *

Thème 4 — Simulation et optimisation
de systèmes complexes
Projet Ondes

Rapport de recherche n° 4962 — Octobre 2003 — 32 pages

Abstract: Thanks to the use of the Cagniard-De Hoop method, we derive an analytic solution in the time domain for the half-space problem associated with the wave equation with Engquist-Majda higher order boundary conditions. This permits us to derive new convergence results when the order of the boundary condition tends to infinity, as well as error estimates. The theory is illustrated by numerical results.

Key-words: Cagniard-De Hoop method, Absorbing boundary conditions, Wave equation, Error estimates, Convergence, Green's function.

* INRIA, Domaine de Voluceau, B.P.105 78153 Le Chesnay Cedex, France

Unité de recherche INRIA Rocquencourt
Domaine de Voluceau, Rocquencourt, BP 105, 78153 Le Chesnay Cedex (France)
Téléphone : +33 1 39 63 55 11 — Télécopie : +33 1 39 63 53 30

Une analyse des conditions absorbantes d'ordre élevé pour l'équation des ondes

Résumé : Nous obtenons, grâce à la méthode de Cagniard-De Hoop, une solution analytique temporelle pour le problème de l'équation des ondes dans le demi-espace avec les conditions aux limites absorbantes d'ordre élevé d' Engquist-Majda. Ceci nous permet d'obtenir de nouveaux résultats de convergence quand l'ordre de la condition aux limites tend vers l'infini ainsi que des estimations d'erreur. La théorie est illustrée par des résultats numériques.

Mots-clés : Méthode de Cagniard-De Hoop, Conditions aux limites absorbantes, Equation des ondes, Estimation d'erreur, Convergence, Fonction de Green.

Table of Contents

1 Introduction

The design of accurate absorbing boundary conditions for the numerical calculation of waves in the time domain is already an old subject since the major work of Engquist and Majda [11], [12] has been achieved at the end of the 70's. Their main contribution was the construction and analysis of a hierarchy of local boundary conditions for the wave equation. Let us concentrate ourselves on the 2D acoustic wave equation:

$$\frac{1}{c^2}\frac{\partial^2 u}{\partial t^2} - \Delta u = 0, \quad x = (x_1, x_2) \in \mathbb{R}^2, \quad t > 0. \tag{1.1}$$

Assuming that the data (initial data) of the problem are supported in the upper half-space $\mathbb{R}^2_+ = \{x_2 > 0\}$, it is natural to try to reduce the effective numerical computations to this half-space by imposing adequate absorbing boundary conditions on the artificial boundary $\Gamma = \partial\mathbb{R}^2_+$. In [11], B. Engquist and A. Majda proposed the following condition (the integer N is a parameter devoted to be large):

$$\mathcal{B}^N u = 0, \quad \text{on } \Gamma, \tag{1.2}$$

where the operators

$$\mathcal{B}^N = \mathcal{B}^N(\frac{\partial}{\partial t}, \frac{\partial}{\partial x_1}, \frac{\partial}{\partial x_2}), \quad N \geq 0,$$

are a family of homogeneous differential operator defined inductively by:

$$\begin{cases} \mathcal{B}^0 = I, \quad \mathcal{B}^1 = \dfrac{\partial}{\partial t} - c\,\dfrac{\partial}{\partial x_2}, \\ \mathcal{B}^{N+1} = \dfrac{\partial}{\partial t}\,\mathcal{B}^N - \dfrac{c^2}{2}\dfrac{\partial^2}{\partial x_1^2}\,\mathcal{B}^{N-1}. \end{cases} \tag{1.3}$$

Note that $\mathcal{B}^N$ can be rewritten in the form:

$$\mathcal{B}^N = S_{N-1}(\frac{\partial}{\partial t}, \frac{\partial}{\partial x_1})\,\frac{\partial}{\partial x_2} - Q_N(\frac{\partial}{\partial t}, \frac{\partial}{\partial x_1})$$

where Q_N and S_{N-1} are homogeneous polynomials of two variables of respective degrees N and $N-1$. In particular, $\mathcal{B}^N$ remains of first order with respect to x_2 ; the condition (1.2) can be

seen as a Dirichlet to Neumann (or impedance) type boundary condition since it can be formally rewritten as:

$$\frac{\partial u}{\partial x_2} - \frac{Q_N(\frac{\partial}{\partial t}, \frac{\partial}{\partial x_1})}{S_{N-1}(\frac{\partial}{\partial t}, \frac{\partial}{\partial x_1})}\, u = 0 \tag{1.4}$$

Remark 1.1 *For smooth solutions (up to the boundary Γ) of the wave equation, the boundary condition (1.2) can be rewritten in terms of t and x_2 derivatives only. Indeed, $\mathcal{B}^N$ is obviously even with respect to the x_1 variable and, thanks to the wave equation, the second order derivative with respect to x_1 can be replaced by t and x_2 derivatives:*

$$\frac{\partial^2}{\partial x_1^2} \longrightarrow \frac{1}{c^2}\frac{\partial^2}{\partial t^2} - \frac{\partial^2}{\partial x_2^2}.$$

As a consequence, one can show that [22]:

$$\mathcal{B}^N u = 0 \quad \Longleftrightarrow \quad \widetilde{\mathcal{B}}^N u = 0, \quad \widetilde{\mathcal{B}}^N = (\frac{\partial}{\partial t} - c\frac{\partial}{\partial x_2})^N. \tag{1.5}$$

This remark will be useful in section 3.

Let us recall that the Initial-boundary value problems for linear hyperbolic systems (1.2), or (1.4) or (1.5), is constructed as an approximation of an exact or transparent boundary condition

$$\mathcal{B} u = 0, \quad \mathcal{B} = \frac{\partial}{\partial x_2} - \mathcal{L}, \tag{1.6}$$

where $\mathcal{L}$ is a pseudo-differential operator in (x_1, t) whose symbol is known explicitly. More precisely, if one uses the Laplace-Fourier transform in the (t, x_1) plane (see (3.3) and (3.2)):

$$\varphi(x_1, t) \rightarrow \widetilde{\varphi}(k, s),$$

one has the formula:

$$\widetilde{\mathcal{L}\,\varphi}(k,s) = (k^2 + \frac{s^2}{c^2})^{\frac{1}{2}}\, \varphi(k,s), \quad \mathcal{R}e\, (k^2 + \frac{s^2}{c^2})^{\frac{1}{2}} \geq 0. \tag{1.7}$$

This comes from the fact that if u is solution of the wave equation in the lower half-space $\mathbb{R}^2_- = \{x_2 < 0\}$ with zero initial data, its partial Laplace-Fourier transform in t and x_1, $\widetilde{u}(k, x_2, s)$, satisfies:

$$\widetilde{u}(k, x_2, s) = \widetilde{u}(k, 0, s)\, e^{(k^2 + \frac{s^2}{c^2})^{\frac{1}{2}}\, x_2}, \quad x_2 \leq 0,$$

which yields in particular:

$$\frac{d\widetilde{u}}{dx_2}(k, 0, s) - (k^2 + \frac{s^2}{c^2})^{\frac{1}{2}}\, \widetilde{u}(k, 0, s) = 0.$$

The presence of the square root in the symbol of $\mathcal{L}$ makes the operator $\mathcal{L}$, and consequently the boundary condition (1.6), non local in space and time, which is a priori very unpleasant from the numerical point of view. The approximate condition simply comes from a rational approximation of the symbol of $\mathcal{L}$ in such a way that the resulting boundary condition can be expressed in terms of differential operators, which is much more tractable from the numerical point of view. If one writes:

$$(k^2 + \frac{s^2}{c^2})^{\frac{1}{2}} = \frac{s}{c}\, (1 + \frac{c^2 k^2}{s^2})^{\frac{1}{2}},$$

the problem is reduced to the rational approximation of the function of one variable:

$$f(z) = (1+z^2)^{\frac{1}{2}}.$$

Noticing that $f(z)$ is a solution of the fixed point equation:

$$f(z) = 1 + \frac{z^2}{1+f(z)}, \tag{1.8}$$

one obtains a rational approximation (or continuous fraction expansion) of $f(z)$ with the following fixed point algorithm:

$$f_{n+1}(z) = 1 + \frac{z^2}{1+f_n(z)}, \quad f_1(z) = 1. \tag{1.9}$$

The condition (1.2) is obtained by replacing in (1.6) $\mathcal{L}$ by $\mathcal{L}_N$ whose symbol is $\frac{s}{c}\, f_N(\frac{ck}{s})$. It is then relatively easy to deduce the induction formula (1.3) from (1.9).

Remark 1.2 *It is easy to show that the sequence $f_n(z)$ converges, for large n, to $f(z)$ only if $|z| < 1$. Moreover, the convergence is uniform and exponential in any compact of the unit circle. For $|z| < 1$, $f_n(z)$ converges to $-f(z)$ which is the other solution of (1.8). However, this is not a problem for the application to absorbing boundary conditions as it will be shown in this paper.*

It is also well known that (1.9) provides the sequence of $\{p,p\}$ (for even n) and $\{p+1,p\}$ (for odd n) Padé approximants [3] of $f(z)$ at the neighborhood of the origin:

$$f_1(z) = 1 + \frac{z^2}{2}, \quad f_2(z) = 1 + \frac{2z^2}{4+z^2}, ...$$

and in particular one has:

$$f_n(z) - f(z) = O\left((z^2)^N\right), \quad z \to 0, \tag{1.10}$$

That is why the boundary condition (1.2) is known as the Engquist-Majda condition of order $2m$. (1.10) shows that the rational approximation of the symbol of $\mathcal{L}$ given by (1.9) privileges the small values of ck/s which has a physical interpretation (see below).

During the past years, an abundant research has been devoted to various improvements (including in particular "better" rational approximations) and extensions (including in particular the application to other wave equations) of the Engquist-Majda conditions. It is not possible to give here an exhaustive bibliography and we will refer the reader to recent review papers on the subject by Hagström [17], [18] and Givoli [13]. In the last decade, alternative solutions have been progressively developed and especially, people have tried to promote again the use of exact non local boundary either by using specific geometries for the absorbing boundaries, as in the works by Gröte-Keller [14], [15] or by exploiting the recent progress in rapid algorithms (multi-pôles) and rational approximation, as in the work of Alpert-Greengard-Hagström [2], [1]. Approximately at the same period, the introduction by J.P. Bérenger of the Perfectly Mached Layers (PML's) technique [5], [6] has partly revolutionnarized the subject. The philosophy here is to replace the absorbing boundary by an absorbing layer (or sponge layer) who has the astonishing property to generate no reflection at the interface between the propagative medium and the absorbing one. This method has rapidly attracted a lot of people in different fields of application, in particular for its good practical performances and its easy implementation.

All these methods (local higher order ABC's, non local ABC's and PML's) have been successfully introduced in a number of different computational codes. Of course, for anybody who wants to use such codes, the natural question is : which is the best method for the absorption of waves.

Our feeling is that there is no universal answer to such a question and that a response should include some criteria : nature of the problem to be adressed, accuracy, speed of calculation, easyness of the implementation, long time behaviour,... However, even with given criteria, the answer would be delicate, in particular because no complete and fair comparison has been done between the three classes of methods. The first reason, which is easy to understand, is that there is probably nobody in the world who has implemented the three methods with the same amount of care. The second reason is a lack of analysis, which is hard in particular if one is interested in getting convincing error estimates. The objective of the present paper is to fill partially this lack in the theory in the case of higher order local absorbing conditions.

Of course, there is a lot of available theoretical results about higher order absorbing boundary conditions. The first question that was raised by Engquist and Majda in their original papers was the one of the well posedness of the initial boundary value problem (IBVP) "wave equation - ABC". This is not a trivial question since it is known that polynomial approximations of degree greater than 2 of the function $f(z)$ (as for instance the successive Taylor approximations of f around 0) give rise to strongy ill-posed problems. However, thanks to the well known Kreiss theory (the so called normal mode analysis [25], [21]), the stability theory of higher order ABC's is more or less completely understood. In particular, necessary and sufficient conditions have been given in [26] about the rational approximations of $f(z)$ in order to ensure the strong well-posedness of the corresponding IBVP (of course, the approximations f_n given by (1.9) fulfill these conditions, as already observed in [12])) and energy estimates (giving rise to stability results, i.e. a priori estimates independent of N) have been obtained in [8].

Concerning the accuracy of absorbing boundary conditions, the simplest analysis consists in analysing the reflection of plane waves, which amounts to study particular solutions of the form ($k \in \mathbb{R}$ and $\theta \in [-\frac{\pi}{2}, \frac{\pi}{2}]$ are parameters, K is the wave number, while θ represents the angle of incidence of the incident plane wave):

$$u_\theta(x,t) = \exp ik(x_1 \sin\theta - x_2 \cos\theta - ct) + \mathbf{R} \exp ik(x_1 \sin\theta + x_2 \cos\theta - ct), \tag{1.11}$$

where:

- $\exp ik(x_1 \sin\theta - x_2 \cos\theta - ct)$ is the incident wave,
- $\exp ik(x_1 \sin\theta + x_2 \cos\theta - ct)$ is the incident wave, R being the reflection coefficient.

By construction, (1.11) is a solution of the wave equation (1.1). It remains to determine $\mathbf{R}$ in order to satisfy the boundary condition (1.2). The computations show that $\mathbf{R}$ only depends on the angle of incidence θ:

$$\mathbf{R} = \mathbf{R}_N(\theta) \equiv \frac{(f_N - f)(\sin\theta)}{(f_N + f)(\sin\theta)} = (-1)^N \left(\frac{1-\cos\theta}{1-\cos\theta}\right)^N. \tag{1.12}$$

In particular one sees that for any $\theta \in]-\frac{\pi}{2}, \frac{\pi}{2}[$, $\mathbf{R}_N(\theta)$ tends (exponentially fast) to 0 when $N \to +\infty$ while $|\mathbf{R}_N(\pm\frac{\pi}{2})| = 1$ (see also figure 1).
There are much fewer results about convergence and error estimates. In fact, there was no real progress since the initial result of Engquist-Majda, result I am recalling now. They were addressing the following 2D model problem:

$$\begin{cases} \text{Find } v : \mathbb{R}^2_- \times \mathbb{R} \mapsto \mathbb{R} & \text{such that} \\ \dfrac{1}{c^2}\dfrac{\partial^2 v}{\partial t^2} - \Delta v = 0 & \text{in } \mathbb{R}^2_- \times \mathbb{R}^+, \\ v(x_1, 0, t) = g(x_1, t), & \text{on } x_2 = 0, \\ v(x,t) = 0, & \text{for } t < 0. \end{cases} \tag{1.13}$$

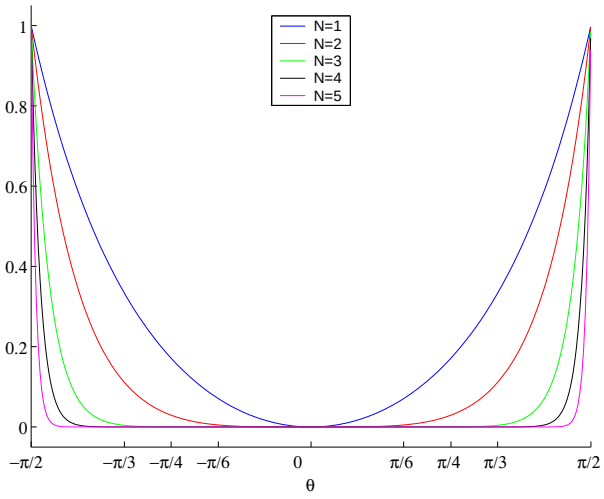

Figure 1: The reflection coefficient

One wishes to get a good approximation of v in a domain $\Omega_b = \{x \ / \ -b < x_2 < 0\}$, for given $b > 0$ by putting an absorbing boundary condition on the line $x_2 = -a$, with $a > b$:

$$
\left\{
\begin{array}{ll}
\text{Find } v^N : \Omega_a \times \mathbb{R} \mapsto \mathbb{R} & \text{such that} \\
\dfrac{1}{c^2}\dfrac{\partial^2 v^N}{\partial t^2} - \Delta v^N = 0 & \text{in } \Omega_a \times \mathbb{R}^+, \\
v^N(x_1, 0, t) = g(x_1, t), & \text{on } x_2 = 0, \\
\mathcal{B}^N v^N = 0, & \text{on } x_2 = -a, \\
v^N(x, t) = 0, & \text{for } t < 0.
\end{array}
\right. \tag{1.14}
$$

In (1.14) there are two important parameters, the order N of the boundary condition and the distance a from the source g to the interface. One assumes that the function g is square integrable in both space and time:

$$
\int_0^{+\infty} \int_{\mathbb{R}} \mid g(x_1, t) \mid^2 dx_1 dt < +\infty. \tag{1.15}
$$

Theorem 1.1 *[12] For any $\varepsilon > 0$ and any arbitrarily large integer M, there exist $N_0 = N_0(\varepsilon, M)$ and $a_0 = a_0(\varepsilon, M)$ such that, for any $N \geq N_0$ and $a \geq a_0$:*

$$
\int_0^T \int_{\Omega_b} \mid (v - v^N)(x, t) \mid^2 dx\ dt < \varepsilon, \quad \forall\, T \leq Ma. \tag{1.16}
$$

- This result is only a convergence result and does not provide an error estimate. Thus it is not a guide for choosing in practice N and a.
- The fact that the result is valid for any time interval of the form $[0, Ma]$ indicates that the result takes into account an arbitrary large number of reflections on the absorbing boundary.
- Which is not satisfactory with theorem 1.1 is the fact that the estimate (1.16) requires a to be sufficiently large. In particular, this does not provide a convergence result when $N \to +\infty$ for fixed a.

- Looking at the proof of theorem enlightens the need for a sufficiently large. It is not our purpose to reproduce here the proof, but it seems useful to emphasize some points. The idea is to use the Fourier transform in space and time:

$$v(x_1, x_2, t) \to \widetilde{\mathbf{v}}(k, x_2, \omega) = \widetilde{v}(k, x_2, i\omega).$$

One can get an explicit solution for both $\widetilde{\mathbf{v}}$ and $\widetilde{\mathbf{v}}^N$. In particular, we have:

$$\left| \begin{array}{l} \widetilde{\mathbf{v}}(k, x_2, \omega) = \widetilde{\mathbf{g}}(k, \omega)\ \exp(\xi^2 - \omega^2/c^2)^{\frac{1}{2}} \cdot x_2 \\ \\ (\xi^2 - \omega^2/c^2)^{\frac{1}{2}} = \left\{ \begin{array}{ll} \sqrt{\xi^2 - \omega^2/c^2} & \text{if } \xi^2 \geq \omega^2/c^2, \\ \\ i\sqrt{\omega^2/c^2 - \xi^2} & \text{if } \xi^2 \leq \omega^2/c^2. \end{array} \right. \end{array} \right.$$

In particular:

  - If $\xi^2 < \omega^2/c^2$, the function $x_2 \to \widetilde{\mathbf{v}}(k, x_2, \omega)$ is oscillating : this is the region of propagative modes.
  - If $\xi^2 < \omega^2/c^2$, the function $x_2 \to \widetilde{\mathbf{v}}(k, x_2, \omega)$ is exponentially decaying when $x_2 \to -\infty$: this is the region of evanescent modes.

When one looks at the error $e^N = v^N - v$, its Fourier transform appears as a sum (the sum is a priori infinite but becomes finite if one is interested in times less than Ma) over $j \geq 1$ of terms of the form:

$$\mathcal{R}_N(\frac{c\,\xi}{\omega})^{\,j}\ \cdot\ \widetilde{\mathbf{g}}(k, \omega)\ \cdot\ \exp\left[(\xi^2 - \omega^2/c^2)^{\frac{1}{2}}\ (\pm x_2 + 2ja)\right].$$

where the *reflection coefficient* $\mathcal{R}_N$ is given by:

$$\mathcal{R}_N(\nu) = \frac{(f_N - f)(\nu)}{(f_N + f)(\nu)} \tag{1.17}$$

and satisfies:

$$\left\{ \begin{array}{l} \mathcal{R}_N(\sigma) \leq 1, \quad \text{(stability result)}, \\ \\ \mathcal{R}_N(\sigma) \to 0, \quad \text{for } |\sigma| < 1, \quad \text{(cf. remark 1.2)}. \end{array} \right.$$

Up to technical details (this is in particular where the assumption (1.15) intervenes), the idea of the proof is the following:

  - In the propagative region $\xi^2 < \omega^2/c^2$, $|\mathcal{R}_N(\sigma)|^{\,j}$ can be made arbitrarily small by choosing N large enough.
  - In the evanescent region $\xi^2 > \omega^2/c^2$, $|\exp\left[(\xi^2 - \omega^2/c^2)^{\frac{1}{2}}\ (\pm x_2 + 2ja)\right]|$ can be made arbitrarily small by choosing a large enough.

One then concludes with Plancherel's theorem.

Physically, the fact that $f_n(z)$ has nothing to do with $f(z)$ for $|z| > 1$ means that the evanescent modes are not correctly taken into account by the absorbing condition. This is why one needs to have a large enough in order to "kill" the amplitude of the evanescent modes at the boundary $x_2 = a$.

In 1988, Halpern and Rauch proposed a high frequency analysis in [19]. More recently, an advance has been achieved by T. Hagström (see [16] or [17]) who derive an approximation theory for the approximation of (a class of) pseudo-differential operators, with the aim to apply it to absorbing

boundary conditions, based on a new reinterpretation of (1.2) and standard quadrature theory. His result, unfortunately, was not transformed into error estimates for absorbing boundary conditions but it gave the clear feeling that it should be possible to obtained convergence resultas by only making N go to $+\infty$ (i.e. without touching the position of the boundary), at least as far as finite times are concerned. This is precisely what we are going to show.

The history of the present work is the following. The Cagniard-De Hoop method is particularly well known in the physics and engineering communities for calculating analytical solutions of time dependent wave propagation problems, especially in seismology (see [7], [24], [23]). This method permits moreover to establish a link between time domain solutions and harmonic plane waves. Trying to learn something about this method (for a completely different problem), we immediately realized that it could easily be applied to the problem of absorbing boundary conditions and would probably help to get new error estimates. The computations are so simple that it is rather surprising to see that nobody did them before, to our knowledge. The object of this article is the presentation of the results we have obtained with this method. We also think that this is a useful tool to teach this subject.

The outline of the paper is as follows. In section 2, we describe the model problem we are dealing with (the half-space problem with a point source) and state our two main results : theorem 2.1 which provides an explicit solution of the corresponding fundamental solution and theorem 2.2 which provides error estimates in the case of a general source function. These two results show that one can get a convergence result only by letting N go to $+\infty$. In some sense, this shows that the need for large a in theorem 1.1 is due to the technique used in the proof but does not correspond to a necessity. However, our results in theorems 2.1 and 2.2 show that increasing the distance from the source to the absorbing boundary helps to get better error estimates. We also pay an attention to large time behaviour of the error, which has already been the subject of previous research works ([10], [9], [4]). Sections 3 and 4 are devoted to the proofs of theorems 2.1 and 2.2. In section 5, we analyse our results in more details and make the confrontation between numerical results and (quasi) analytical results.

2 Main results

The first result of this paper is an explicit expression of the fundamental solution of the 2D wave equation in the half-space $\mathbb{R}^+_2 = \{x_2 > 0\}$ with higher order absorbing boundary conditions on $\Gamma = \{x_2 = 0\} (= \partial\mathbb{R}^+_2)$. Since the problem in invariant under translations in the x_1-direction we can restrict ourselves to the case where the source point is:

$$x_S = (0, h) \quad \text{with } h > 0. \tag{2.1}$$

The problem we want to solve is:

$$\begin{cases} \text{Find } u : \mathbb{R}^2_+ \times \mathbb{R} \mapsto \mathbb{R} & \text{such that} \\ \dfrac{1}{c^2}\dfrac{\partial^2 u}{\partial t^2} - \Delta u = \delta(x - x_S) \times \delta(t) & \text{in } \mathbb{R}^2_+, \\ \mathcal{B}^N u = 0, & \text{on } \Gamma, \\ u(x,t) = 0, & \text{for } t < 0. \end{cases} \tag{2.2}$$

To state our result, it is useful to introduce some notation. Let us define the image source point x^*_S by:

$$x^*_S = (0, -h) \tag{2.3}$$

and let us set :

$$r(x) = |x - x_S|, \quad r^*(x) = |x - x_S^*|. \tag{2.4}$$

We also define the function $\theta(x), x \in \mathbb{R}^2_+$ by:

$$\theta(x) \in]-\frac{\pi}{2}, \frac{\pi}{2}[\,, \quad x - x_S^* = (\, r^*(x)\sin\theta(x),\ r^*(x)\cos\theta(x)\,)^t, \tag{2.5}$$

and finally the function $\Phi(x,t), x \in \mathbb{R}^2_+, t > 0$, by:

$$\Phi(x,t) = \frac{r^*(x)^2\sin^2\theta(x) - (c^2t^2 - r^*(x)^2)}{r^*(x)^2\sin^2\theta(x) + (c^2t^2 - r^*(x)^2)} = \frac{x_1^2 - (c^2t^2 - r^*(x)^2)}{x_1^2 + (c^2t^2 - r^*(x)^2)}. \tag{2.6}$$

We can notice that:

$$ct > r^*(x) \Longrightarrow |\Phi(x,t)| < 1.$$

Finally, we recall that the Tchebycheff polynomials $P_N(x), N \geq 0$, are defined by:

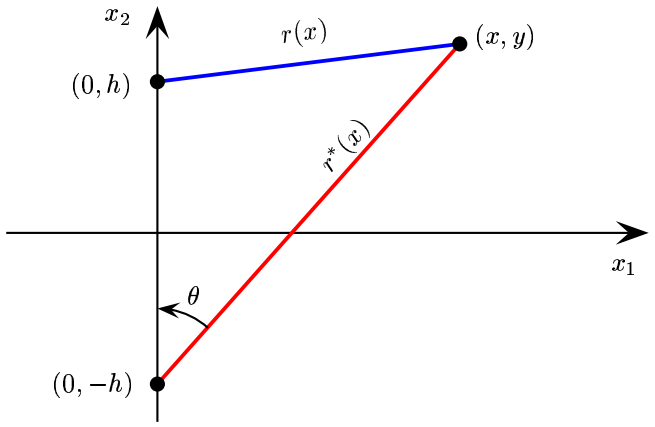

Figure 2: Illustration of the notation

$$P_0(x) = 1, \quad P_1(x) = x, \quad P_{N+1}(x) - 2xP_N(x) + P_{N+1}(x) = 0, \tag{2.7}$$

and satisfy :

$$\forall\, x \in [-1,1], \quad P_N(x) = \cos(\, N\arccos(x)\,). \tag{2.8}$$

In particular, we see that:

$$\forall\, x \in [-1,1], \quad |P_N(x)| \leq 1.$$

Theorem 2.1 *The solution $u(x,t) = G^N(x,t)$ of problem (2.2) is given by:*

$$G^N(x,t) = G_i(x,t) + G_r^N(x,t), \tag{2.9}$$

where, if H denotes the Heaviside function:

$$\left|\begin{array}{l} G_i\,(x,t) = \dfrac{1}{2\pi\sqrt{t^2 - \frac{r(x)^2}{c^2}}}\, H(c\,t - r(x)), \\[2ex] G_r^N(x,t) = \dfrac{P_N\,(\Phi(x,t))}{2\pi\sqrt{t^2 - \frac{r^*(x)^2}{c^2}}} \left[\dfrac{ct - (x_2+h)}{ct + (x_2+h)}\right]^N H(c\,t - r^*(x)). \end{array}\right. \tag{2.10}$$

Remark 2.1 *The function $G_i(x,t)$, which does not depend on N, is nothing but the restriction to the half-space $\mathbb{R}^2_+$ of the fundamental solution of the 2D wave equation in the whole space. That is why it is called the incident field. Conversely, the field $G_r^N(x,t)$, due to the presence of the boundary Γ, is called the reflected field, which does depend on N.*

Remark 2.2 *The presence of the factor $H(c\,t - r^*(x))$ indicates that the reflected field $G_r^N(.,t)$ is compactly supported in the set $\Omega(t) = \Omega_1(t) \cup \Omega_2(t)$ (see definition 4.6).*

Let us now consider the approximation, in the upper half-space of the solution u of the 2D wave equation with "smooth" point source :

$$
(2.11) \qquad \begin{cases} \text{Find } u : \mathbb{R}^2 \times \mathbb{R}^+ \mapsto \mathbb{R} & \text{such that} \\ \\ \dfrac{1}{c^2}\dfrac{\partial^2 u}{\partial t^2} - \Delta u = \delta(x - x_S) \times f(t) & \text{in } \mathbb{R}^2 \times \mathbb{R}^+, \\ \\ u(x,0) = 0, \quad \dfrac{\partial u}{\partial t}(x,0) = 0 & \text{in } \mathbb{R}^2, \end{cases}
$$

where we assume that the source function $f(t)$ is bounded and has support $[0,T]$ (T can be equal to $+\infty$ which includes the case of a permanent source term), by the solution u^N of the boundary value problem:

$$
(2.12) \qquad \begin{cases} \text{Find } u^N : \mathbb{R}^2 \times \mathbb{R}^+ \mapsto \mathbb{R} & \text{such that} \\ \\ \dfrac{1}{c^2}\dfrac{\partial^2 u^N}{\partial t^2} - \Delta u^N = \delta(x - x_S) \times f(t), & \text{in } \mathbb{R}^2 \times \mathbb{R}^+, \\ \\ \mathcal{B}^N u^N = 0, & \text{on } \Gamma, \\ \\ u(x,0) = 0, \quad \dfrac{\partial u}{\partial t}(x,0) = 0 & \text{in } \mathbb{R}^2. \end{cases}
$$

Theorem 2.2 *At each point $x \in \mathbb{R}^2_+$, one has the pointwise estimates:*

- *For $\dfrac{r^*(x)}{c} \le t \le \dfrac{r^*(x)}{c} + T \quad (\Leftrightarrow x \in \Omega_1(t)$ - see (4.6)),*

$$
(2.13) \qquad |u(x,t) - u^N(x,t)| \le \frac{1}{2\pi}\left(\frac{ct - (x_2+h)}{ct + (x_2+h)}\right)^N Log\left(\frac{ct + \sqrt{c^2t^2 - r^*(x)^2}}{r^*(x)}\right) \|f\|_{L^\infty}
$$

- *For $t > \dfrac{r^*(x)}{c} + T \quad (\Leftrightarrow x \in \Omega_1(t)$ - see (4.6)),*

$$
(2.14) \qquad |u(x,t) - u^N(x,t)| \le \frac{1}{2\pi}\left(\frac{ct - (x_2+h)}{ct + (x_2+h)}\right)^N Log\left(\frac{ct + \sqrt{c^2t^2 - r^*(x)^2}}{c(t-T) + \sqrt{c^2(t-T)^2 - r^*(x)^2}}\right) \|f\|_{L^\infty}
$$

Moreover, one has the uniform estimates:

- *For $\dfrac{h}{c} \le t \le \dfrac{h}{c} + T$,*

$$
(2.15) \qquad \|(u - u^N)(.,t)\|_{L^\infty(\mathbb{R}^2_+)} \le \frac{1}{2\pi}\left(\frac{ct - h}{ct + h}\right)^N Log\left(\frac{t + \sqrt{t^2 - (h/c)^2}}{(h/c)}\right) \|f\|_{L^\infty}
$$

- *For* $t > \dfrac{h}{c} + T$,

$$\|(u-u^N)(.,t)\|_{L^\infty(\mathbb{R}^2_+)} \leq \frac{1}{2\pi}\left(\frac{ct-h}{ct+h}\right)^N Log\left(\frac{t+\sqrt{t^2-(t-T)^2}}{t-T}\right)\|f\|_{L^\infty} \tag{2.16}$$

These results appeal the following comments:

- The error converges spectrally to 0 (in the uniform norm) when N goes to infinity.
- For given t, the upper bounds in the estimates (2.15) and (2.16) diminish when the distance h from the source to the absorbing boundary increases. This is coherent with the physical intuition and numerical observations.
- Concerning the behaviour of the error for large t, if we assume that $T < +\infty$, we observe that the right hand side in the estimate (2.16) behaves for large t as

$$\frac{1}{2\pi}\sqrt{\frac{2T}{t}},$$

which shows that, for all N and h, the error converges uniformly to 0 when t tends to $+\infty$. On the other hand, when $T = +\infty$, the right hand side in the estimate (2.15) behaves as

$$\frac{1}{2\pi}\,\mathrm{Log}\; t,$$

which a priori authorizes a logarithmic growth on the error when t tends to $+\infty$. This is what happens if $f(t)$ is for instance the Heaviside function.

Remark 2.3 *We have chosen here to analyse the approximation of a problem associated to a point source. It would not be difficult to adapt theorem 2.2 (or more precisely its proof) to treat the case of a distributed source term $f(x,t)$ or non zero initial data u_0 and u_1. In the same way, we have chosen to present L^∞ estimates, which seemed to us as more pertinent in practice. However, once again, it is easy to adapt the proof in order to get L^p or energy estimates.*

3 Proof of Theorem 2.1

As we already said, the formula ((2.9),(2.10)) results directly from the application of the Cagniard-De Hoop method to problem (2.2). In order to make this paper easily understandable by a reader which is not familiar with this technique, we detail the proof (only some explicit calculations will be omitted). Let us decompose the solution u of (2.2) as:

$$u = G_i + u^r$$

where G_i, given by (2.10), is the fundamental solution of the 2D wave equation. By linearity, it is clear that u^r satisfies:

$$\left\{\begin{array}{ll} \text{Find } u^r : \mathbb{R}^2_+ \times \mathbb{R} \mapsto \mathbb{R} & \text{such that} \\ \dfrac{1}{c^2}\dfrac{\partial^2 u^r}{\partial t^2} - \Delta u^r = 0 & \text{in } \mathbb{R}^+_2, \\ \mathcal{B}^N u^r = -\mathcal{B}^N G_i, & \text{on } \Gamma, \\ u(x,t) = 0, & \text{for } t < 0\ . \end{array}\right. \tag{3.1}$$

We apply successively to u^r:

- The Laplace transform in time (s is the dual variable of t):

$$\widetilde{u}^r(x_1, x_2, s) = \int_0^{+\infty} u^r(x_1, x_2, t)\, e^{-st}\, dt, \tag{3.2}$$

- The Fourier transform in the tangential space variable x_1 (k is the dual variable of x_1):

$$\widehat{u}^r(k, x_2, s) = \int_{-\infty}^{+\infty} \widetilde{u}^r(x_1, x_2, s)\, e^{ikx_1}\, dx_1. \tag{3.3}$$

The algorithm for applying the Cagniard-De Hoop method is the following:

1. Compute explicitly $\widehat{u}^r(k, x_2, s)$.
2. Apply the inverse Fourier transform in x_1:

$$\widetilde{u}^r(x_1, x_2, s) = \frac{1}{2\pi} \int_{-\infty}^{+\infty} \widehat{u}^r(k, x_2, s)\, e^{-ikx_1}\, dx_1, \tag{3.4}$$

3. Transform (by means of complex analysis methods) the integral (3.4) into an integral of the form:

$$\widetilde{u}^r(x_1, x_2, s) = \int_0^{+\infty} F(x_1, x_2, t)\, e^{-st}\, dt, \tag{3.5}$$

Then, by surjectivity of the Laplace-Fourier transform, we shall have identified the solution (compare (3.2) and (3.5)):

$$u^r(x_1, x_2, t) \equiv F(x_1, x_2, t). \tag{3.6}$$

The first step is straightforward. From the wave equation, we deduce that the function $x_2 \mapsto \widehat{u}^r(k, x_2, s)$ satisfies:

$$-\frac{d^2\widehat{u}^r}{dx_2^2} + (k^2 + \frac{s^2}{c^2})\, \widehat{u}^r = 0.$$

Retaining only the solutions that decay when $x_2 \to +\infty$ for $\mathcal{R}e(s) \geq 0$, we deduce the existence of a complex valued function $A(k, s)$ such that:

$$\widehat{u}^r(k, x_2, s) = A(k, s)\, e^{-(k^2+s^2)^{\frac{1}{2}} x_2}, \tag{3.7}$$

where we have chosen to use the determination of the complexe square root corresponding to:

$$\forall\, z \in \mathbb{C}, \quad \mathcal{R}e\, z^{\frac{1}{2}} \geq 0, \tag{3.8}$$

which corresponds to make coïncide the branch cut of $z^{\frac{1}{2}}$ with the semi real axis $\mathcal{I}m\ z = 0$, $\mathcal{R}e\ z < 0$. Since $u^r + G_i$ is smooth for $y < h$, we can use the fact that:

$$\mathcal{B}^N(u^r + G_i) = 0 \Longleftrightarrow (\frac{1}{c}\frac{\partial}{\partial t} - \frac{\partial}{\partial x_2})^N\, (u^r + G_i) = 0, \quad \text{for } x_2 = 0. \tag{3.9}$$

On the other hand, it is well known that the Laplace-Fourier transform of G_i is given by:

$$\widehat{G}_i(k, x_2, s) = \frac{e^{-(k^2+\frac{s^2}{c^2})^{\frac{1}{2}}|x_2 - h|}}{2(k^2 + \frac{s^2}{c^2})^{\frac{1}{2}}}. \tag{3.10}$$

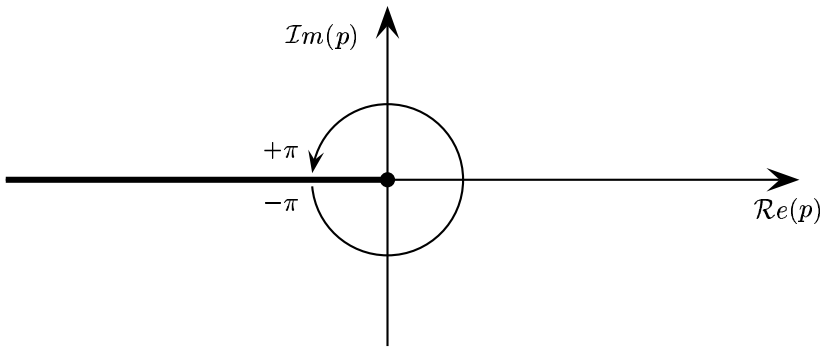

Figure 3: The branch cut for the determination of the complex square root

Taking into account the form (see (3.7) and (3.10)) of $\widehat{u}^r$ and $\widehat{G}_i$, the boundary condition (3.9) leads to :

$$\left(\frac{s}{c}+(k^2+\frac{s^2}{c^2})^{\frac{1}{2}}\right)^N A(k,s)+\frac{1}{2}\left(\frac{s}{c}-(k^2+\frac{s^2}{c^2})^{\frac{1}{2}}\right)^N e^{-(k^2+\frac{s^2}{c^2})^{\frac{1}{2}}h}=0,$$

This permits us to compute $A(k,s)$ and finally to get:

$$\widehat{u}^r(k,x_2,s)=R^N(k,\frac{s}{c})\,\frac{e^{-(k^2+\frac{s^2}{c^2})^{\frac{1}{2}}(x_2+h)}}{2(k^2+\frac{s^2}{c^2})^{\frac{1}{2}}}\ , \tag{3.11}$$

where we have set:

$$R^N(k,\sigma)=\mathcal{R}_N(\frac{k}{\sigma})\left[\frac{\sigma-(k^2+\sigma^2)^{\frac{1}{2}}}{\sigma+(k^2+\sigma^2)^{\frac{1}{2}}}\right]^N. \tag{3.12}$$

Therefore (this is step 2) we have:

$$\widetilde{u}^r(x_1,x_2,s)=\frac{1}{4\pi}\int_{-\infty}^{+\infty}R^N(k,\frac{s}{c})\,\frac{e^{-(k^2+\frac{s^2}{c^2})^{\frac{1}{2}}(x_2+h)}}{(k^2+\frac{s^2}{c^2})^{\frac{1}{2}}}\,e^{-ikx_1}\,dk, \tag{3.13}$$

that we would like to transform into an integral of the form (3.5) (this is step 2). This is the part of the approach which is specific to the Cagniard-De Hoop method. We are helped by the following facts:

- The integrand in (3.13) is homogeneous in s and k.
- The dependence with respect to x_2 of this integrand is exponential.

First, exploiting the homogeneity property, we apply the change of variable $k=ps/c$ and obtain:

$$\widetilde{u}^r(x_1,x_2,s)=\frac{1}{4\pi}\int_{-\infty}^{+\infty}R^N(p,1)\,\frac{e^{-s\,[\,(1+p^2)^{\frac{1}{2}}(\frac{x_2+h}{c})+ip\frac{x_1}{c}\,]}}{(1+p^2)^{\frac{1}{2}}}\,dp,\quad(\equiv\int_{-\infty}^{+\infty}\Psi(p)\,dp). \tag{3.14}$$

In the sequel we fix $(x_1,x_2)\in\mathbb{R}^2_+$ with $x_1>0$ (which is not restrictive since the solution we are looking for is clearly even in x_1). We introduce $r^*=r^*(x)$ and $\theta=\theta(x)$ ($\in[0,\pi/2]$ since $x_1\geq 0$) according to the definitions (2.4) and (2.5). We thus have:

$$\begin{cases} x_1=r^*\sin\theta,\\ \\ x_2+h=r^*\cos\theta. \end{cases} \tag{3.15}$$

Now the idea is to consider the variable p as a complex variable and to see the integral (3.14) as a contour integral, the contour coïnciding with the real axis. If one is able, by a contour deformation, to transform this integral into a contour integral on some curve Γ along which one can use a parametric representation of the form:

$$(1+p^2)^{\frac{1}{2}}\,(\frac{x_2+h}{c}) + ip\frac{x_1}{c} = t, \quad \text{for } t>0, \tag{3.16}$$

we shall have reached our goal. To achieve this, we first remark that the integrand $\Psi(p)$ in (3.14) is an analytic function of p if one excepts the two branch cuts constituted of the two half-lines of purely imaginary numbers whose modulus is greater than ct/r^* (see figure 4). Then, we introduce the so-called Cagniard-De Hoop contour Γ defined as:

$$\begin{cases} \Gamma = \Gamma^+ \cup \Gamma^- \ , \\ \\ \Gamma^\pm = \{\ p = \gamma^\pm(t) \equiv -i\,\dfrac{ct}{r^*}\cos\theta \pm |\sin\theta|\,\sqrt{\dfrac{c^2t^2}{r^{*2}}-1}, \quad t \geq \dfrac{r^*}{c}\}. \end{cases} \tag{3.17}$$

It is clear that the two curves $\Gamma^\pm$ are symmetric the one from the other with respect to the imaginary axis, and meet at point $-i\cos\theta$ (for $t = r^*/c$). More precisely, it is easy to check that Γ is nothing but the branch of the hyperbola of equation:

$$\frac{Y^2}{\cos^2\theta} - \frac{X^2}{\sin^2\theta} = \frac{1}{c^2}, \quad (p = X+iY,\ (X,Y)\in \mathbb{R}^2),$$

which is located in the upper half-space $Y = \mathcal{I}m\ p > 0$. Note that this hyperbola does not intersect the two branch cuts of Ψ. All this information is summarized in figure 4.

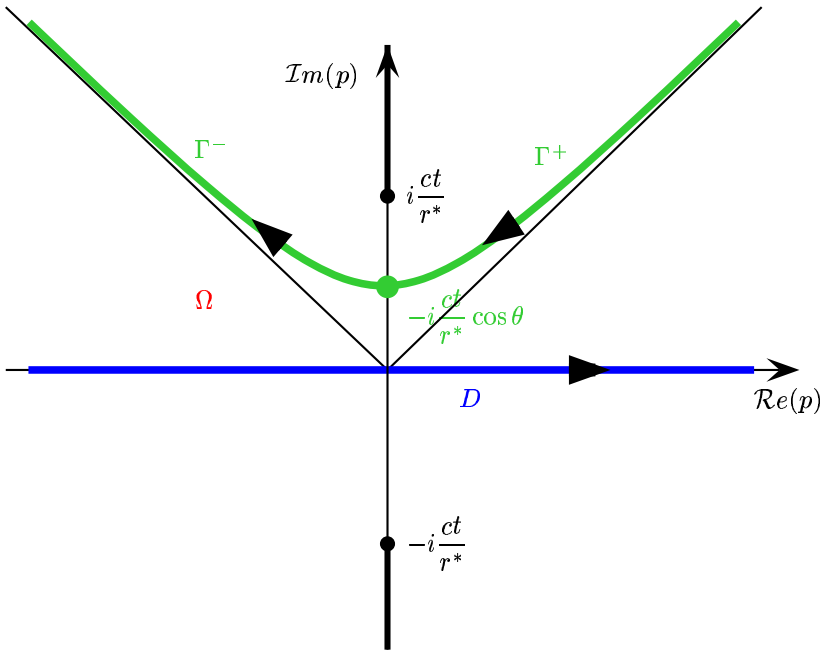

Figure 4: The contours Γ and D

In fact, to understand where (3.17) comes from, it suffices to remark that $\gamma^\pm(t)$ are nothing but than the two roots of the equation (3.16), considered as an equation in p (the calculations are left

to the reader).

Let us denote by D the real line and by Ω the connected part of the complex plane delimited by D and Γ. Let $\rho > 0$ a parameter devoted to tend to $+\infty$. We set:

$$\left| \begin{array}{l} D_\rho = \{p \in D \ / \ |p| \leq \rho\}, \quad \Gamma_\rho = \{p \in \Gamma \ / \ |p| \leq \rho\}, \\ \\ C_\rho = \{p \in \Omega \ / \ |p| = \rho\}. \end{array} \right.$$

Note that C_ρ is made of two arcs of the circle of center 0 and radius ρ that join D_ρ to Γ_ρ in such

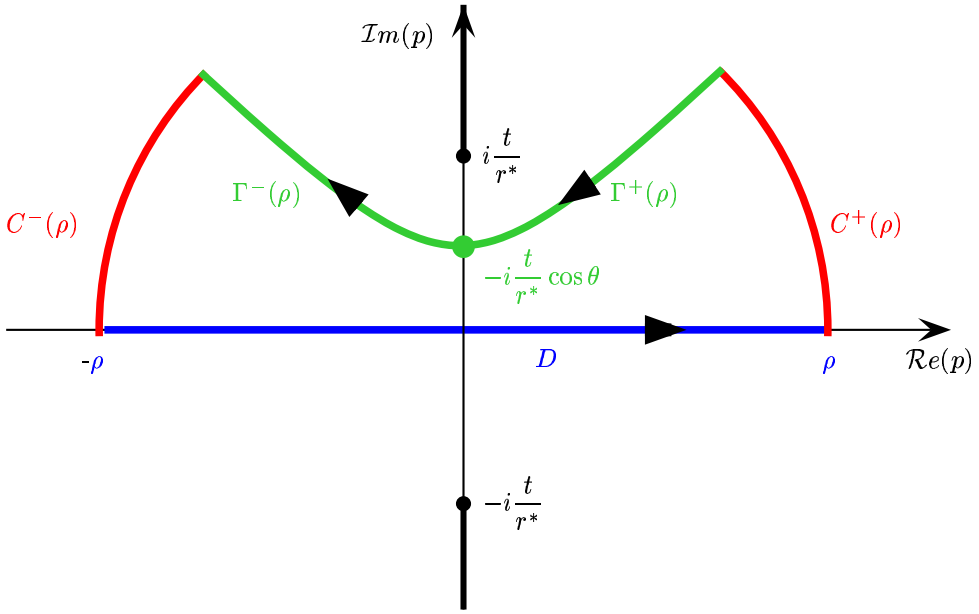

Figure 5: The closed contour $D_\rho \cup C_\rho \cup \Gamma_\rho$

a way that $D_\rho \cup C_\rho \cup \Gamma_\rho$ is a closed curve. Since $\Psi(p)$ is analytic in Ω, the integral of Ψ along $D_\rho \cup C_\rho \cup \Gamma_\rho$ (we choose the orientation of this path such that the real segment is described in the sense of increasing values - see figure 5) is identically 0 (Jordan's lemma):

$$\int_{D_\rho} \Psi(p)\, dp + \int_{C_\rho} \Psi(p)\, dp + \int_{\Gamma_\rho} \Psi(p)\, dp = 0.$$

Thanks to the choice of the square root and since $x_2+h > 0$, the function $\Psi(p)$ decays exponentially to 0 when $\mathcal{I}m\ p$ goes to $+\infty$. As a consequence, it is easy to show that:

$$\lim_{\rho \to +\infty} \int_{C_\rho} \Psi(p)\, dp = 0.$$

Therefore, from (3.14), we deduce:

$$\widetilde{u}^r(x_1, x_2, s) = \frac{1}{4\pi} \int_\Gamma R^N(p,1)\, \frac{e^{-s\,[\,(1+p^2)^{\frac{1}{2}}(\frac{x_2+h}{c}) + ip\frac{x_1}{c}\,]}}{(1+p^2)^{\frac{1}{2}}}\, dp.$$

We use the parametrizations $p = \gamma^+(t)$ and $p = \gamma^-(t)$, for $t \geq R$, respectively along Γ^+ and Γ^- and remark that:

$$\left| \begin{array}{ll} \bullet\ (1+p^2)^{\frac{1}{2}}(\dfrac{x_2+h}{c}) + ip\dfrac{x_1}{c} = t, & \text{(by construction)}, \\ \bullet\ \dfrac{dp}{(\frac{1}{c^2}+p^2)^{\frac{1}{2}}} = \pm\dfrac{dt}{(t^2-\frac{r^{*2}}{c^2})^{\frac{1}{2}}}, & \text{on } \Gamma^{\pm}. \end{array} \right.$$

Therefore, since t goes from $+\infty$ to 0 on Γ^+ and from 0 to $+\infty$ on Γ^- :

$$\widetilde{u}^r(x_1,x_2,s) = \frac{1}{4\pi}\int_0^{+\infty} \left[R^N(\gamma^+(t),1) + R^N(\gamma^-(t),1)\right] \frac{e^{-st}}{(t^2-\frac{r^{*2}}{c^2})^{\frac{1}{2}}}\, dt.$$

Finally, observing that $\gamma^-(t)^2 = \overline{\gamma^+(t)}^2$ and using the fact that $\sqrt{\overline{z}} = \overline{\sqrt{z}}$, we deduce that:

$$R^N(\gamma^-(t),1) = \overline{R^N(\gamma^+(t),1)} \Longrightarrow R^N(\gamma^+(t),1) + R^N(\gamma^-(t),1) = 2\,\mathcal{R}e\ \left[R^N(\gamma^+(t),1)\right],$$

which yields

$$\widetilde{u}^r(x_1,x_2,s) = \frac{1}{2\pi}\int_{\frac{r^*}{ct}}^{+\infty} \mathcal{R}e\ \left[R^N(\gamma^+(t),1)\right] \frac{e^{-st}}{(t^2-\frac{r^{*2}}{c^2})^{\frac{1}{2}}}\, dt. \tag{3.18}$$

Thanks to formula (3.12), one has:

$$R^N(\gamma^+(t),1) = \left[R^1(\gamma^+(t),1)\right]^N, \tag{3.19}$$

while one easily computes that:

$$R^1(\gamma^+(t),1) = \frac{r^* - ct\cos\theta + i\sin\theta\sqrt{c^2t^2-r^{*2}}}{r^* + ct\cos\theta - i\sin\theta\sqrt{c^2t^2-r^{*2}}} = \rho_1(t)\ e^{i\alpha(t)}.$$

Setting $\Phi = \Phi(x,t)$ (cf. (2.6)), one finds that (the calculations - rather tedious but straightforward - are left to the reader) :

$$\left\{ \begin{array}{l} \rho_1(t) = \dfrac{ct - r^*\cos\theta}{ct + r^*\cos\theta} = \dfrac{ct-(x_2+h)}{ct+(x_2+h)}, \\ \cos\alpha(t) = \dfrac{r^{*2}\sin^2\theta - (c^2t^2-r^{*2})}{r^{*2}\sin^2\theta + (c^2t^2-r^{*2})} = \Phi. \end{array} \right.$$

Therefore, according to (3.19):

$$\mathcal{R}e\ \left[R^N(\gamma^+(t),1)\right] = \rho_1(t)^N\cos\left(N\alpha(t)\right),$$

that is to say, since $\alpha(t) = \arccos\Phi$:

$$\mathcal{R}e\ \left[R^N(\gamma^+(t),1)\right] = \left[\frac{ct-(x_2+h)}{ct+(x_2+h)}\right]^N P_N(\Phi)\ . \tag{3.20}$$

It is the easy to conclude from (3.18) and (3.20).

4 Proof of Theorem 2.2

Let u and u^N be the respective solutions of (2.11) and (2.12). We introduce the error (or reflected field) e^N defined as:

$$e^N = u^N - u. \tag{4.1}$$

To get the pointwise estimates (2.13) and (2.14), we fix $x \in \mathbb{R}^2_+$ and set $r^* = r^*(x)$ and $\theta = \theta(x)$. Obviously $e^N(x,t) = 0$ for $t \leq r^*/c$ while, for $t > r^*/c$, we deduce from theorem 2.1 that:

$$e^N(x,t) = \int_{\max(\frac{r^*}{c},\, t-T)}^{t} G_r^N(x,\tau)\; f(t-\tau)\; d\tau, \quad t \geq \frac{r^*}{c}, \tag{4.2}$$

using that f is supported in $[0,T]$ and $G_r^N(x,.)$ in $[0,\frac{r^*}{c}]$. We deduce that:

$$\begin{cases} |e^N(x,t)| \leq \|f\|_{L^\infty(0,t)} \;\cdot\; \|G_r^N(x,.)\|_{L^1(\frac{r^*}{c},t)} & \text{if } \dfrac{r^*}{c} \leq t \leq \dfrac{r^*}{c} + T, \\ |e^N(x,t)| \leq \|f\|_{L^\infty(0,T)} \;\cdot\; \|G_r^N(x,.)\|_{L^1(t-T,t)} & \text{if } t > \dfrac{r^*}{c} + T. \end{cases} \tag{4.3}$$

We thus have to estimate L^1-norms in time of $G_r^N(x,.)$. Using the fact that $|P_N(\Phi(x,t))| \leq 1$ (estimate which is quasi-optimal for a range of values of t) we get :

$$|G_r^N(x,t)| \leq \frac{1}{2\pi\sqrt{t^2 - \frac{(r^*)^2}{c^2}}} \left(\frac{ct - (x_2+h)}{ct + (x_2+h)}\right)^N.$$

We remark that, for $t \geq \dfrac{r^*}{c}$, the function $ct \mapsto \left(\dfrac{ct-(x_2+h)}{ct+(x_2+h)}\right)$ is increasing. Therefore:

$$\begin{aligned} \|G_r^N(x,.)\|_{L^1(\frac{r^*}{c},t)} &\leq \frac{1}{2\pi}\left(\frac{ct-(x_2+h)}{ct+(x_2+h)}\right)^N \int_{\frac{r^*}{c}}^{t} \frac{d\tau}{\sqrt{t^2 - \frac{r^{*2}}{c^2}}}, \\ &= \frac{1}{2\pi}\left(\frac{ct-(x_2+h)}{ct+(x_2+h)}\right)^N \mathrm{Log}\left(\frac{ct + \sqrt{c^2t^2 - r^{*2}}}{r^*}\right) \end{aligned} \tag{4.4}$$

while, as soon as $t > \dfrac{r^*}{c} + T$,

$$\begin{aligned} \|G_r^N(x,.)\|_{L^1(t-T,t)} &\leq \frac{1}{2\pi}\left(\frac{ct-(x_2+h)}{ct+(x_2+h)}\right)^N \int_{t-T}^{t} \frac{d\tau}{\sqrt{t^2 - \frac{r^{*2}}{c^2}}}, \\ &= \frac{1}{2\pi}\left(\frac{ct-(x_2+h)}{ct+(x_2+h)}\right)^N \mathrm{Log}\left(\frac{ct + \sqrt{c^2t^2 - r^{*2}}}{c(t-T) + \sqrt{c^2(t-T)^2 - r^{*2}}}\right). \end{aligned} \tag{4.5}$$

It is easy to deduce (2.13) and (2.14) from (4.3), (4.4) and (4.5).

We now pass to proof of the uniform estimates (2.15) and (2.16). Let us introduce the two disjoint sets:

$$\begin{aligned} \Omega_1(t) &= \{x \in R^2_+ \;/\; c(t-T) < r^*(x) \leq ct\} \\ \Omega_2(t) &= \{x \in R^2_+ \;/\; r^*(x) \leq c(t-T)\} \end{aligned} \tag{4.6}$$

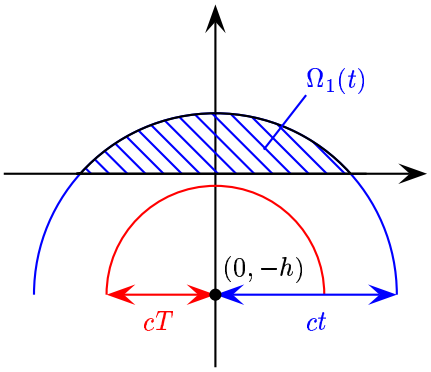

Figure 6: The set $\Omega_1(t), \frac{h}{c} \leq t < \frac{h}{c} + T$

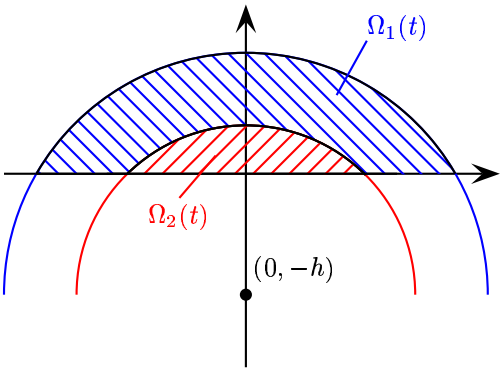

Figure 7: $\Omega_1(t)$ and $\Omega_2(t), t \geq \frac{h}{c} + T$

These two sets are represented in figure for two values of t. Note that $\Omega_1(t)$ is not empty as soon as $t > \frac{h}{c}$ while $\Omega_2(t)$ is not empty as soon as $t > \frac{h}{c} + T$. According to (4.3), in order to derive an L^∞ estimate of $e^N(.,t)$, we need an upper bound for the quantity:

$$\sup_{x \in \Omega_1(t)} \|G_r^N(x,.)\|_{L^1(\frac{r^*}{c},\, t)} \quad \text{when } t > \frac{h}{c},$$

and for the quantity:

$$\sup_{x \in \Omega_2(t)} \|G_r^N(x,.)\|_{L^1(t-T,\, t)} \quad \text{when } t > \frac{h}{c} + T.$$

We remark that for each $x \in \Omega(t) = \Omega_1(t) \cup \Omega_2(t)$, $h \leq x_2 + h \leq ct$. Therefore, noticing that the function:

$$x \mapsto \frac{ct - x}{ct + x}, \quad x \in [0, ct],$$

is decreasing, we get:

$$\sup_{x \in \Omega_1(t)} \left(\frac{ct - (x_2 + h)}{ct + (x_2 + h)} \right) = \sup_{x \in \Omega_2(t)} \left(\frac{ct - (x_2 + h)}{ct + (x_2 + h)} \right) = \frac{ct - h}{ct + h}. \tag{4.7}$$

On the other hand, using the fact that the two functions:

$$\left| \begin{array}{ll} r \mapsto \dfrac{ct}{r} + \sqrt{\dfrac{c^2t^2}{r^2} - 1}\,, & r \in [0, ct], \\[2ex] r \mapsto \dfrac{ct + \sqrt{c^2t^2 - r^2}}{c(t-T) + \sqrt{c^2(t-T)^2 - r^2}}\,, & r \in [0, c(t-T)], \quad (t > T) \end{array} \right.$$

are respectively decreasing and increasing, we deduce that:

$$\left| \begin{array}{l} \displaystyle\sup_{x \in \Omega_1(t)} \mathrm{Log} \left| \frac{ct}{r^*} + \sqrt{\frac{c^2t^2}{r^{*2}} - 1} \right| = \mathrm{Log} \left(\frac{t + \sqrt{t^2 - (h/c)^2}}{(h/c)} \right), \quad \text{if } \frac{h}{c} < t < \frac{h}{c} + T \\[2ex] \displaystyle\sup_{x \in \Omega_1(t)} \mathrm{Log} \left| \frac{ct}{r^*} + \sqrt{\frac{c^2t^2}{r^{*2}} - 1} \right| = \mathrm{Log} \left(\frac{t + \sqrt{t^2 - (t-T)^2}}{t - T} \right), \quad \text{if } t > \frac{h}{c} + T \end{array} \right.$$

$$\sup_{x\,\in\,\Omega_2(t)} \mathrm{Log}\left|\frac{ct+\sqrt{c^2t^2-r^{*2}}}{c(t-T)+\sqrt{c^2(t-T)^2-r^{*2}}}\right| = \mathrm{Log}\left(\frac{t+\sqrt{t^2-(t-T)^2}}{t-T}\right)\ , \quad \text{if } t>\frac{h}{c}+T$$

These last three equalities, together with (4.3), (4.4) and (4.5), permit us to show the inequalities:

$$\sup_{x\,\in\,\Omega_1(t)} \|G_r^N(x,.)\|_{L^1(\frac{r^*}{c},\,t)} \le \frac{1}{2\pi}\left(\frac{ct-h}{ct+h}\right)^N \mathrm{Log}\left(\frac{ct}{h}+\sqrt{\frac{c^2t^2}{h^2}-1}\right) \quad (t>\frac{h}{c}), \tag{4.8}$$

$$\sup_{x\,\in\,\Omega_2(t)} \|G_r^N(x,.)\|_{L^1(t-T,\,t)} \le \frac{1}{2\pi}\left(\frac{ct-h}{ct+h}\right)^N \mathrm{Log}\left(\frac{t+\sqrt{t^2-(t-T)^2}}{t-T}\right) \quad (t>\frac{h}{c}+T). \tag{4.9}$$

It is then easy to conclude from (4.8), (4.9) and (4.3).

Remark 4.1 *In formula (2.10), the function G_r^N naturally appears as the product of 3 terms. In the proof above, in order to estimate G_r^N we have estimated independently, for the sake of simplicity, each of these factors. In particular, our final estimates are not necessarily sharp.*

5 Illustration and analysis of the results

5.1 Analysis of the 2D fundamental solutions

Relative error analysis. One of the difficulty to represent numerically the reflected field G_r^N given by (2.10) is the presence of the singularity of the circle $r^*(x)=ct$. To overcome this difficulty, the idea is to compare this reflected field to what it would be with the Neumann boundary condition (which corresponds to $N=0$). That is why we introduce the relative error field defined as (Note that $G_r^0(.,t)$ does not vanish inside the disk $r^*(x)<ct$):

$$\gamma_r^N(x,t) = \frac{G_r^N(x,t)}{G_r^0(x,t)} = P_N\left(\Phi(x,t)\right)\left[\frac{ct-(x_2+h)}{ct+(x_2+h)}\right]^N, \quad x\in\Omega(t). \tag{5.1}$$

In the following experiments we choose $h=1$ and $c=1$. On figures 8 to 12 we represent, at three different times, namely $t=3,5$ and 7 from top to bottom, the level lines of $x\mapsto\gamma_r^N(x,t)$. Each figure corresponds to one value of N ($N=1,2,5,10,20$) We clearly observe that:

- The amplitude of the error strongly decays with N (take care of the scales). For instance, at $t=3$, the error level is 0.4 for $N=1$, 0.2 for $N=2$, 0.02 for $N=5$, 7.10^{-4} for $N=10$ and 6.10^{-7} for $N=20$.
- As expected, the amplitude of the error also increases in time. By a homogeneity argument, it is obvious that looking at different t for fixed h is equivalent to looking at different h's for fixed t. Therefore, our results also illustrate the influence of h on the reflected field.
- When N increases, the relative error concentrates more and more at the neighrborhood of the absorbing bundary. Moreover, its dependence with respect to the space variable is more and more complicated (this is the effect of the Tchebycheff polynomials).

Study of the error as a function of time. Here we wish to study the evolution of the reflected fiels at a given point x as a function of time. All the points we observe are located on the circle $r^*(x)=5$ so that the reflected field arrives to these points at time $t=5$.

- **The case of the point $\theta(x)=0$.** Contrary to what the plane wave analysis might suggest, the reflected field is not identically 0 for $\theta(x)=0$, i.e on the x_2 axis. However, the function

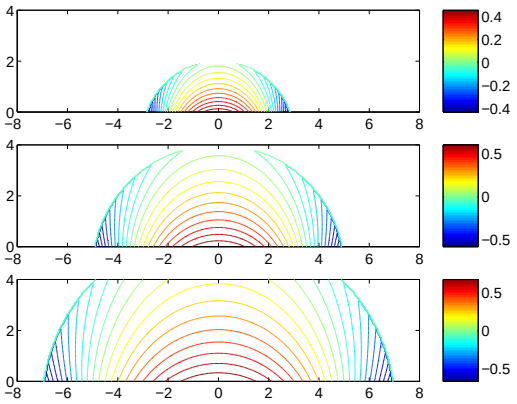

Figure 8: $x \mapsto \gamma_r^1(x,t), t = 3, 5$ and 7

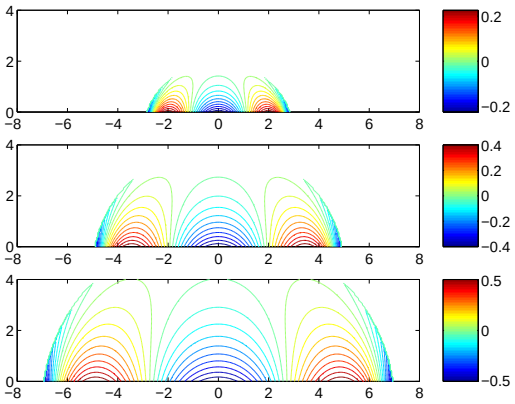

Figure 9: $x \mapsto \gamma_r^2(x,t), t = 3, 5$ and 7

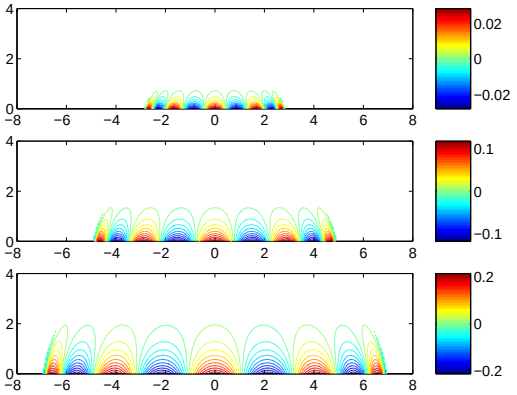

Figure 10: $x \mapsto \gamma_r^5(x,t), t = 3, 5$ and 7

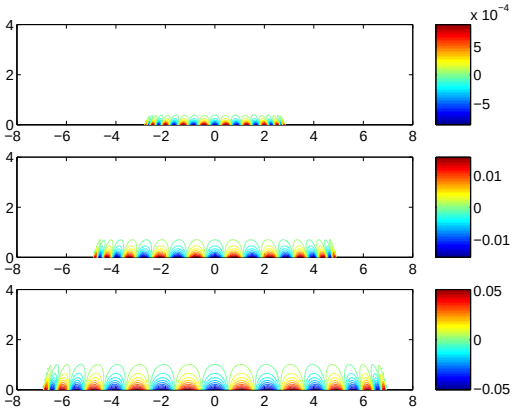

Figure 11: $x \mapsto \gamma_r^{10}(x,t), t = 5, 7$ and 9

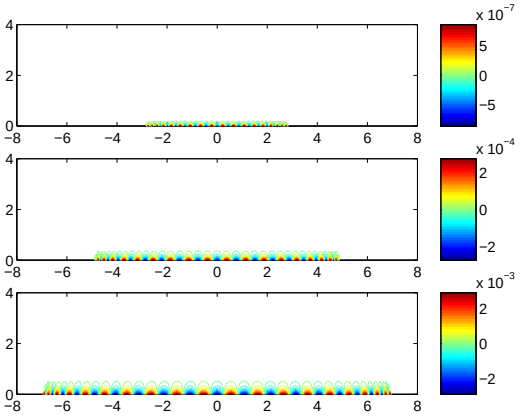

Figure 12: $x \mapsto \gamma_r^{20}(x,t), t = 3, 5$ and 7

$t \mapsto G_r^N(x,t)$ is not discontinuous (except for $N=0$!) at time $t=\tau=\tau(x)=(x_2+h)/c$ as shown by the formula:

$$G_r^N(x,t) = \frac{(-1)^N}{2\pi} \frac{[ct-(x_2+h)]^{N-\frac{1}{2}}}{[ct+(x_2+h)]^{N+\frac{1}{2}}}, \quad \text{for } t>\tau. \tag{5.2}$$

It is even less and less singular when N increases. Moreover, one sees that the function $t \mapsto G_r^N(x,t)$ is increasing from $t=\tau$ to $t=2N\tau$ then decreasing for $t>2N\tau$ and tends to 0 when $t \to +\infty$ as $1/2\pi ct$. The maximum of $t \mapsto G_r^N(x,t)$ is given by:

$$\sup_{t\geq\tau} G_r^N(x,t) = \frac{1}{2N+1}\left(\frac{2N-1}{2N+1}\right)^{N-\frac{1}{2}} \sim \frac{1}{8N} \quad (N \to +\infty) \tag{5.3}$$

These properties are illustrated on figures 5.1 and 5.1, where we represent (on fig 5.1) the variations of $t \mapsto G_r^N(x,t), t \in [0,20]$ for $N=1$ to 5. Looking at the relative error, the

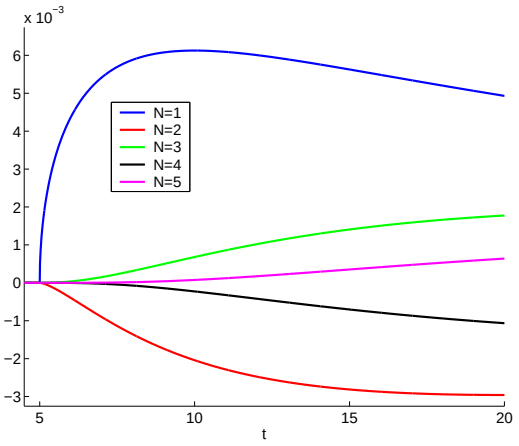

Figure 13: $t \mapsto G_r^N(x,t), r^*=5, \theta=0$

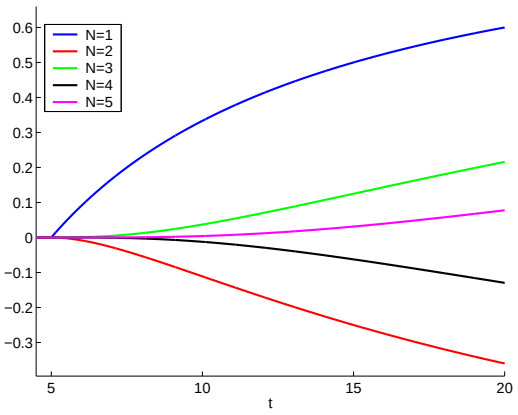

Figure 14: $t \mapsto \gamma_r^N(x,t), r^*=5, \theta=0$

formula:

$$\gamma_r^N(x,t) = \frac{(-1)^N}{2\pi} \frac{[ct-(x_2+h)]^{N-\frac{1}{2}}}{[ct+(x_2+h)]^{N+\frac{1}{2}}}, \quad \text{for } t>\tau. \tag{5.4}$$

shows that the function $t \mapsto \gamma_r^N(x,t), t>\tau$, increases from 0 to $1/2\pi$. This is confirmed on figure 5.1

- **The case of points $\theta(x) \neq 0$.** In this case, the function $t \mapsto \gamma_r^N(x,t)$ is no longer continuous fot $t=\tau$:

$$\lim_{t\to\tau} \gamma_r^N(x,t) = \mathbf{R}_N(\theta(x)) = (-1)^N \left(\frac{1-\cos\theta}{1-\cos\theta}\right)^N. \tag{5.5}$$

On figures 15 and 16 we represent the variations of $t \mapsto \gamma_r^N(x,t)$ for $\theta=\pi/6$ and $\theta=\pi/3$. On each picture, one makes n vary from 1 to N. Clearly, the higher is N, the more the function oscillates. Finally, for large times, one easily computes that:

$$\lim_{t\to+\infty} \gamma_r^N(x,t) = (-1)^N, \tag{5.6}$$

independently of the value of N.

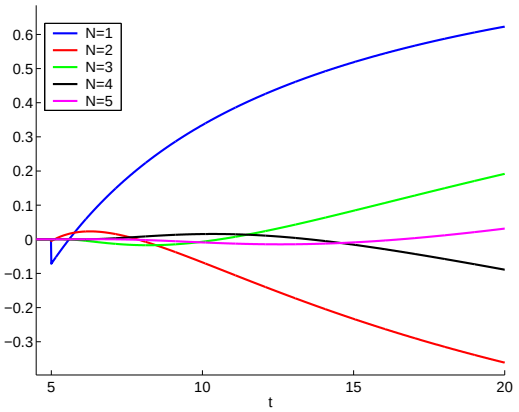

Figure 15: $t \mapsto \gamma_r^N(x,t), r^* = 5, \theta = \frac{\pi}{6}$

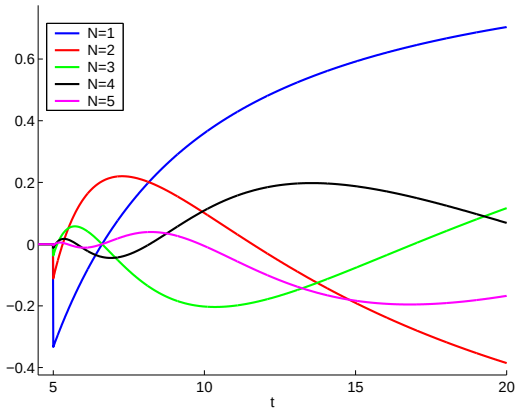

Figure 16: $t \mapsto \gamma_r^N(x,t), r^* = 5, \theta = \frac{\pi}{3}$

Study of the error as a function of the distance to the image source We consider here the spatial variation of the reflected field along a ray, namely the part of a half-line starting from the image source point S^* included in the half space $\mathbb{R}^2_+$. For a given direction $\theta \in]-\pi/2, \pi/2[$, this ray is also defined as:

$$D_\theta = \{x \in \mathbb{R}^2_+ \ / \ \theta(x) = \theta\} = \{(r^* sin\theta, r^* cos\theta), r^* \geq h/\cos\theta$$

In the next figures we represent the variations of the reflected field G_r^N, for fixed θ as a function of $r^* \geq h/\cos\theta$, for different values of t and N.

For $\theta = 0$, $r^* = h = 1$. On figures 17 to 20, we represent the variations of G_r^N along D_0 for 3 values of t, $t = 3, 5, 8$. Each figure corresponds to one value of N, and therefore, the scale varies a lot for one picture to the other. Once again, one observes that the reflected field is smoother and smoother when N increases.

For $\theta = \pi/6$, $r^* = h = 2/\sqrt{3}$. On figures 21 to 24, we represent the variations of G_r^N along $D_{\pi/6}$ for $t = 3, 5, 8$.This time, the functions are singular for $r^* = ct$. However, one observes that the region where G_r^N takes very large values becomes more and more confined close to the point $r^* = ct$ when N increases.

For $\theta = \pi/6$, $r^* = h = 2$. On figures 25 to 28, we represent the variations of G_r^N along $D_{\pi/3}$ for $t = 3, 5, 8$.This time, the functions are singular for $r^* = ct$. The shape of the reflected wave is more complicated than for $\theta = \pi/6$, especially for large N.

Angular variation of the reflected wave. Our previous results have already illustrated the dependence of the reflected field with respect to $\theta(x)$. Here, let us consider the relative error $\gamma_r^N(x,t)$ along the "reflected" wave front defined as:

$$WF_r(t) = \partial\Omega(t) = \{x \in \mathbb{R}^2_+ \ / \ r^*(x) = ct\} \quad (\neq \emptyset \text{ for } t > \frac{h}{c}).$$

Let $M_\theta(t) = (ct\sin\theta, ct\cos\theta) \in WF_r(t)$ (note that $M_\theta(t)$ describes $WF_r(t)$ when θ varies from $-\arccos\frac{h}{ct}$ to $+\arccos\frac{h}{ct}$), one easily deduces from (2.10) that:

$$\lim_{x \to M_\theta(t), x \in \Omega(t)} \gamma_r^N(x,t) = \mathbf{R}_N(\theta) = (-1)^N \left(\frac{1-\cos\theta}{1-\cos\theta}\right)^N.$$

In other words, the curve representing, as a function of the direction θ, the variations of the relative error $\gamma_r^N(x,t)$ along the "reflected" wave front $WF_r(t)$ is nothing but the portion of the curve of figure 1 that corresponds to $-\arccos\frac{h}{ct} \leq \theta \leq \arccos\frac{h}{ct}$.

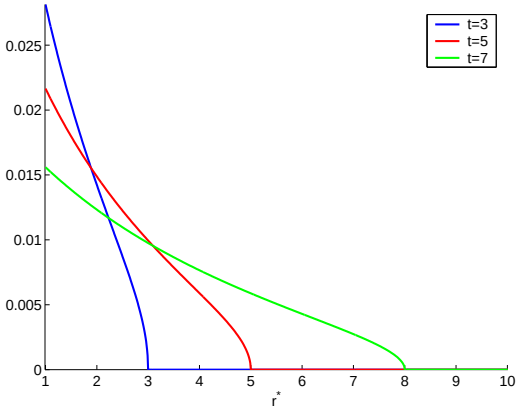

Figure 17: $\theta = 0, N = 1$

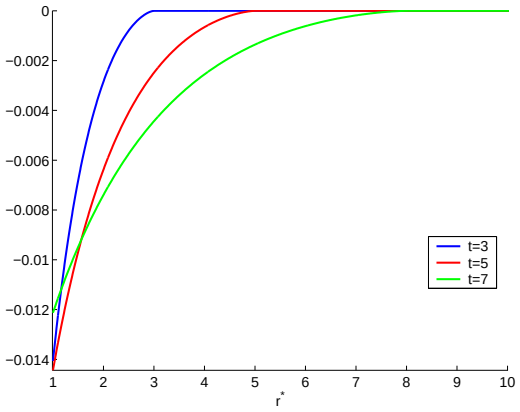

Figure 18: $\theta = 0, N = 2$

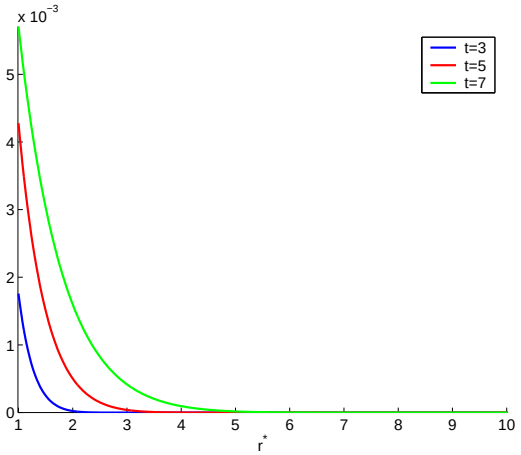

Figure 19: $\theta = 0, N = 5$

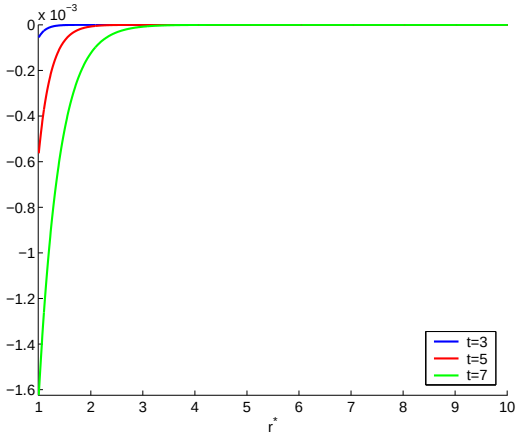

Figure 20: $\theta = 0, N = 10$

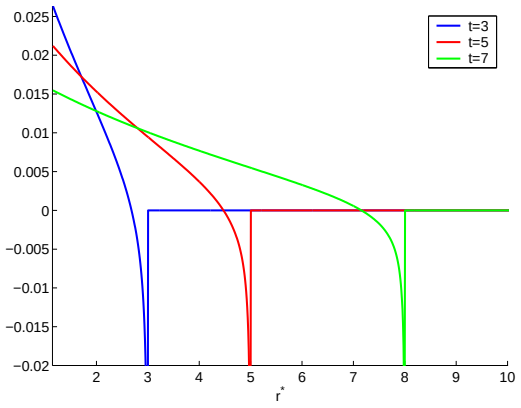

Figure 21: $\theta = \pi/6, N = 1$

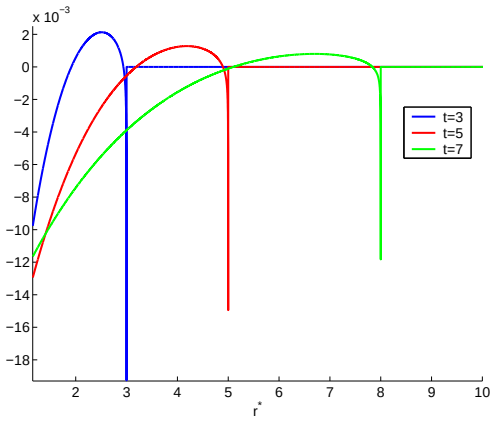

Figure 22: $\theta = \pi/6, N = 2$

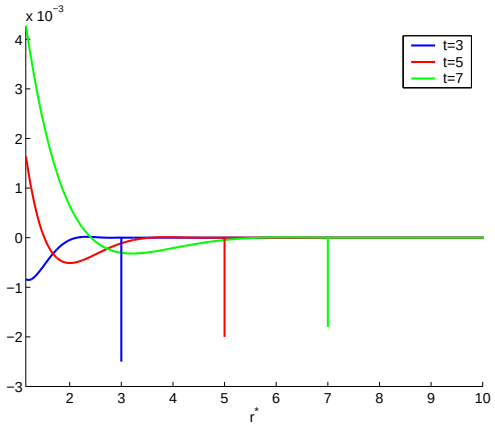

Figure 23: $\theta = \pi/6, N = 5$

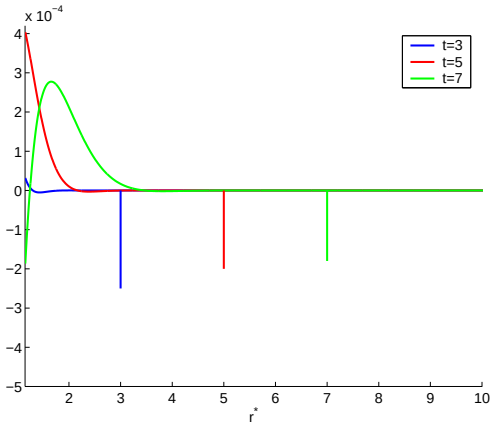

Figure 24: $\theta = \pi/6, N = 10$

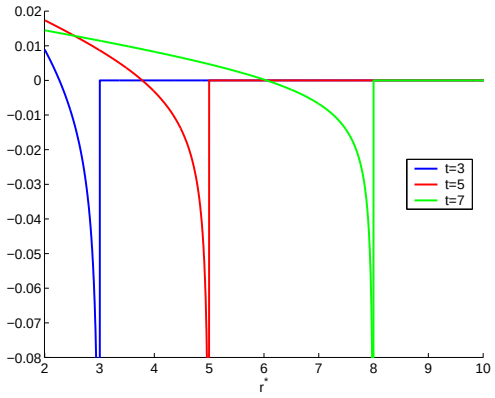

Figure 25: $\theta = \pi/3, N = 1$

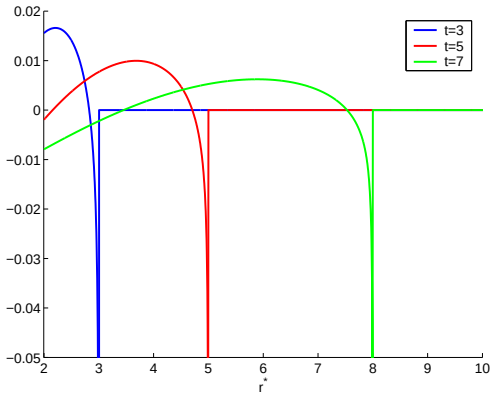

Figure 26: $\theta = \pi/3, N = 2$

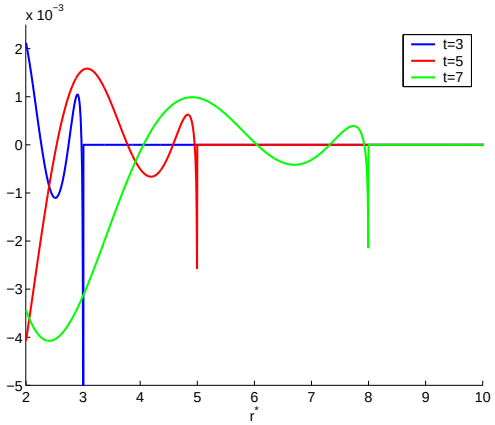

Figure 27: $\theta = \pi/3, N = 5$

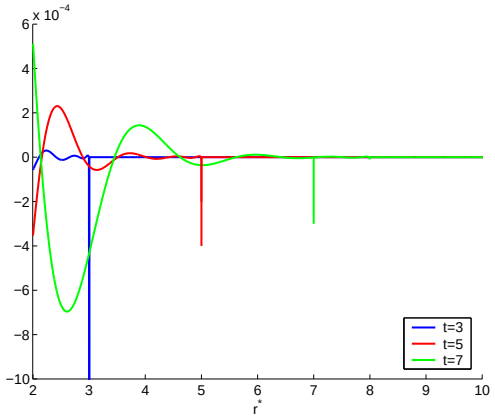

Figure 28: $\theta = \pi/3, N = 10$

5.2 The case of a source term.

Comparison with numerical experiments. We have implemented a MATLAB code for the computation of the convolution integral (4.2). To validate our "exact" solution (!), we have compared our results with those obtained with a finite difference code written by F. Collino. In our experiment, the source function is a truncated first derivative of a Gaussian:

$$f(t) = \frac{d}{dt}\{e^{-2\pi f_0(t-t_0)^2}\}\, H(2t_0 - t), \quad f_0 = 1, t_0 = 1/f_0 \tag{5.7}$$

On figures (29) to (34) we have compared the "analytical" solution (top picture in each figure) to the numerical one (bottom picture in each figure) for three values of N : $N = 1, 3, 5$. In each picture we represent the level lines of the solution at time $t = 0.4$. The left pictures represent the total field while the right pictures represent the reflected field (the error). In each case, for the representation, the reflected field has been amplified by a factor which depends on N : 1.3 for $N = 1$, 10 for $N = 3$, 25 for $N = 5$. In each case, the results reveal a very good agreement between the two solutions. On figures (35) to (40) we have compared both solutions at point $(0.9, 0.1)$ as functions of time. The blue curves represent the "analytical" solution and the red curves the numerical one (bottom picture in each figure) for three values of N: $N = 1, 3, 5$. In each picture we represent the level lines of the solution at time $t = 0.4$. As before the left pictures represent the total field while the right pictures represent the reflected field.

L^∞ error estimates. On figures (41) to (44) we have compared the L_∞ norm of the reflected field (the blue curves) to the uniform estimates (2.16) and (2.16) given by Theorem 2.2 (the red curves) for $N = 1, 2, 5, 10$. The source is a step function in time : $f(t) = 1$ if $0 \leq t \leq 2$ and $f(t) = 0$ otherwise. Our estimate appears to very sharp for $N = 1$ and becomes less accurate (although quite acceptable) when N increases. Since we used the L^∞ norm of the source function to establish our error estimates, one could imagine that this estimate is not very sharp for more complicated source functions. To check this, we have repeted the previous experiment when the source is still given by (5.7) with $f_0 = 1$. Figures (45) to (48) illustrate these experiments for $N = 1, 2, 5, 10$. The estimate is obviously less accurate than in the case of the step source function but still gives a reasonable bound.

6 Conclusion and perspectives

The use of the Cagniard-de Hoop has enabled us to obtain a quasi-analytical representation of the field reflected by the Engquist-Majda's higher order ABC's. This permits us to obtain new theoretical estimates for the time dependent problem.

Of course, the method can be applied to other boundary conditions (we give in appendix the example of Higdon's boundary conditions). It would also be interesting to treat other equations such as Maxwell's equations or elastodynamics equations. One also might think that the Cagniard-de Hoop method could be a new tool for analysing the stability of boundary conditions.

In a forthcoming work, we wish to treat the case of the PML's for absorbing boundary conditions. This should give some insights about the quantitative comparison between ABC's and PML's.

A Extension to Higdon's boundary condtions

In 1986 Higdon [22], [20] proposed another approximation of the condition (1.2) of the form

$$B^N_{Hig} u = \prod_{j=1}^{N} \left(\cos\alpha_j \frac{\partial}{\partial t} - c\, \frac{\partial}{\partial x} \right) u = 0 \tag{A.1}$$

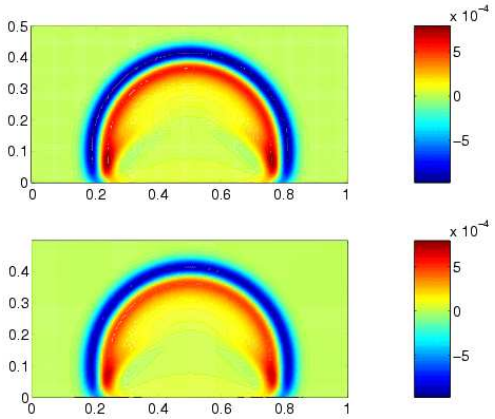

Figure 29: Total field. N=1

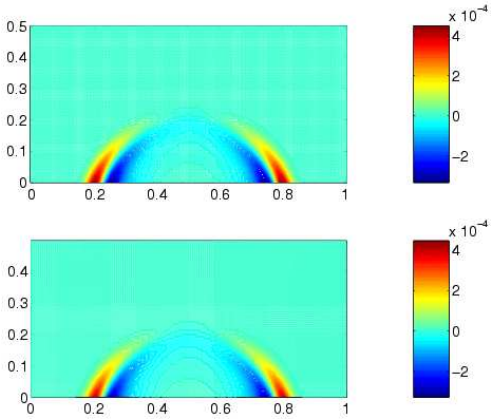

Figure 30: Reflected field. N=1

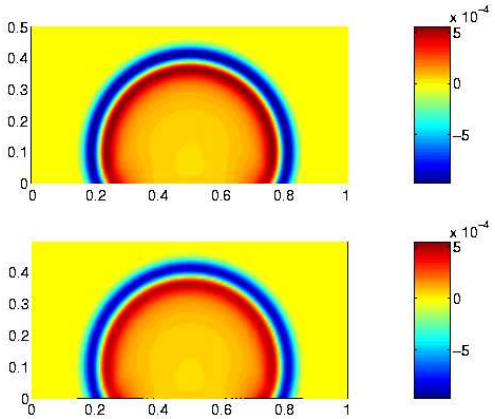

Figure 31: Total field. N=3

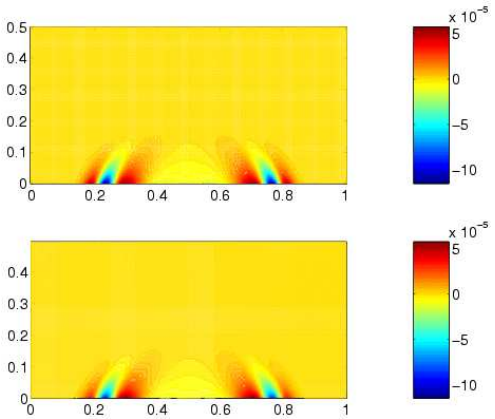

Figure 32: Reflected field. N=3

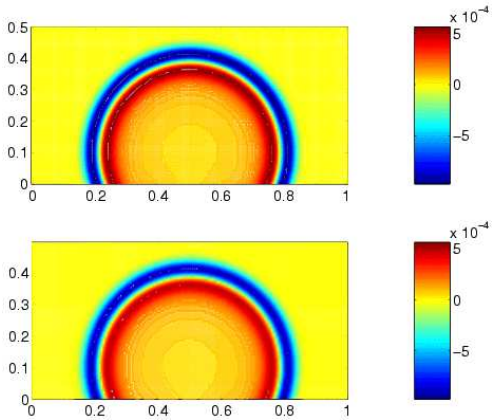

Figure 33: Total field. N=5

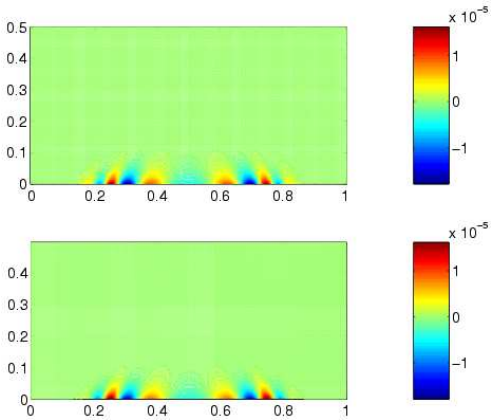

Figure 34: Reflected field. N=5

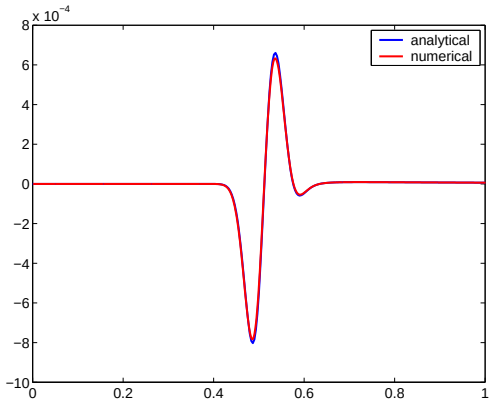

Figure 35: Total field. N=1

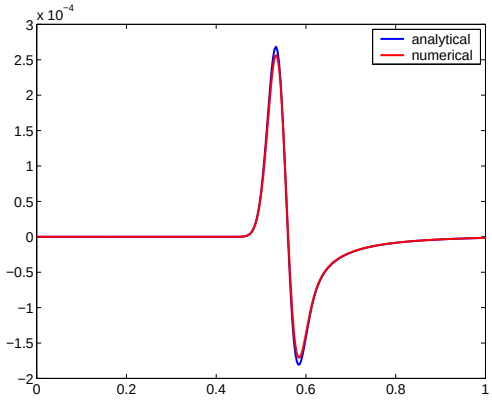

Figure 36: Reflected field. N=1

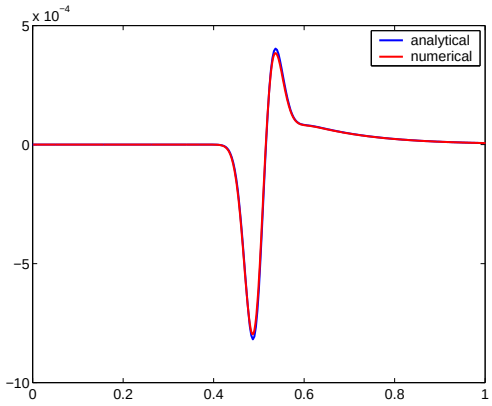

Figure 37: Total field. N=1

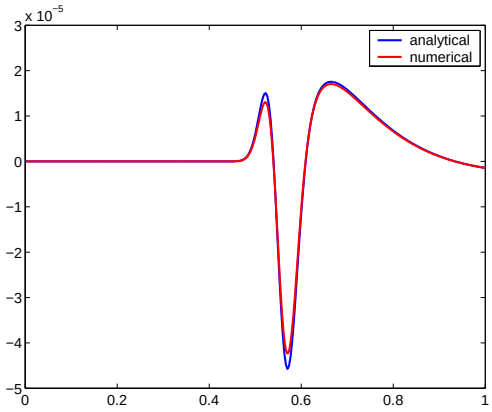

Figure 38: Reflected field. N=1

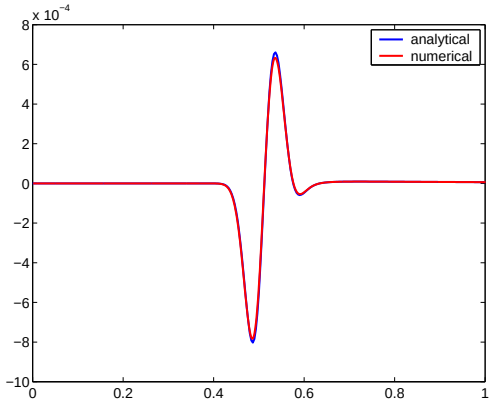

Figure 39: Total field. N=1

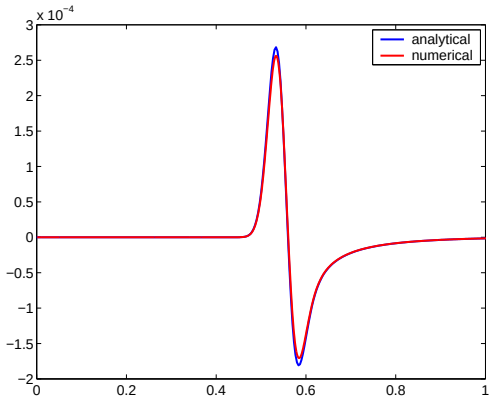

Figure 40: Reflected field. N=1

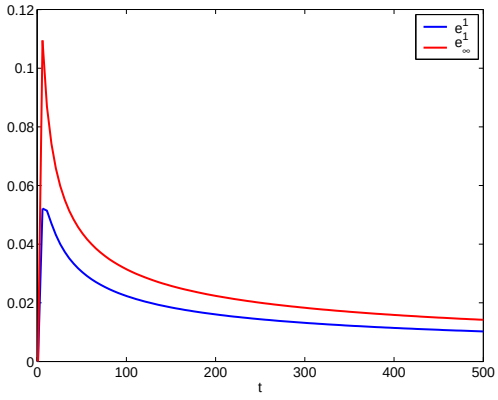

Figure 41: Error estimates N=1

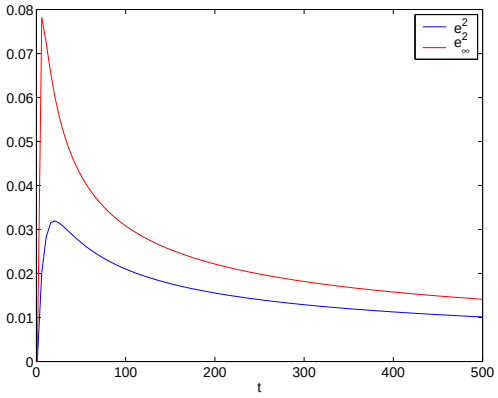

Figure 42: Error estimates N=2

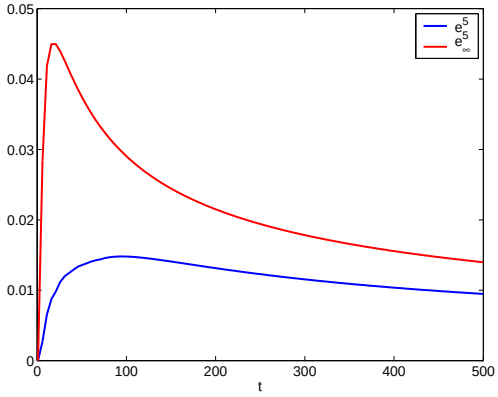

Figure 43: Error estimates N=5

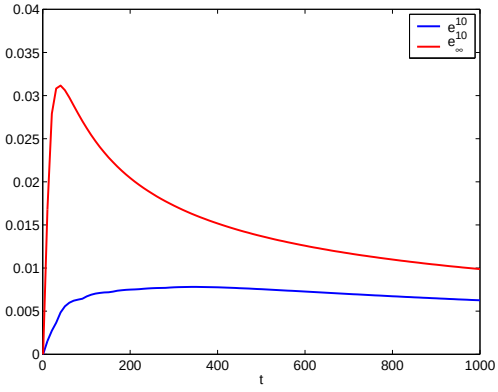

Figure 44: Error estimates N=10

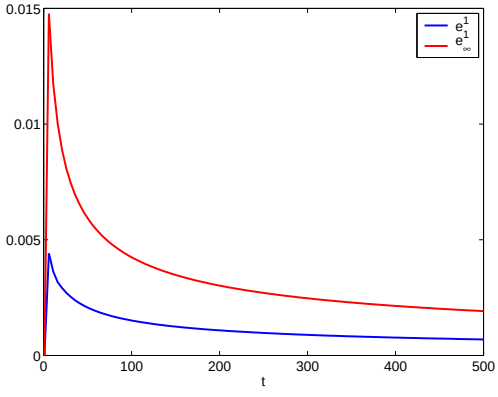

Figure 45: Error estimates N=1

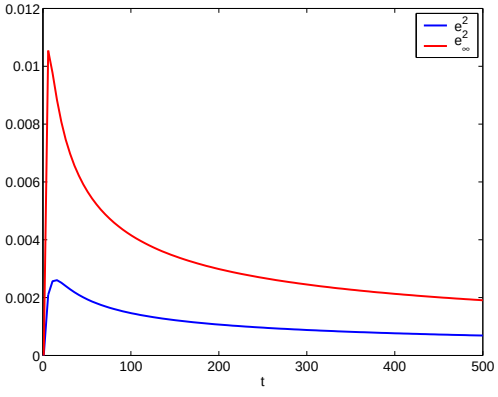

Figure 46: Error estimates N=2

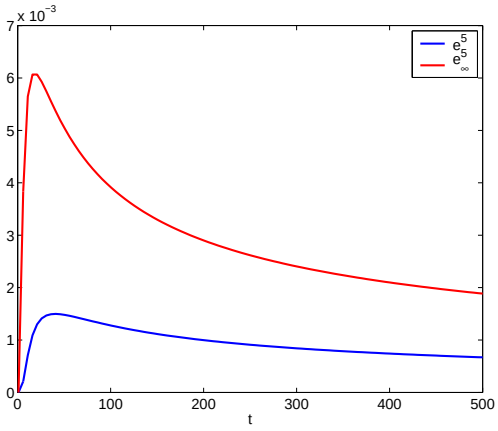

Figure 47: Error estimates N=5

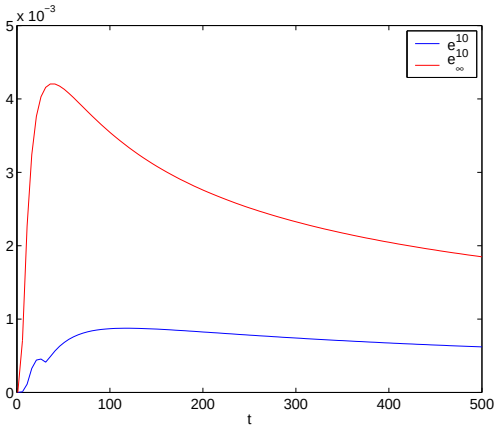

Figure 48: Error estimates N=10

These conditions are a generalization of the condition 1.5 (obtained with $\alpha_j = 0$ for all j) and have the property to be exactly satisfied by any linear combination of plane waves whose angle of incidence is α_j.

Using the same method as in section 3, it can be shown that the solution of the problem

$$\text{(A.2)} \qquad \begin{cases} \text{Find } u : \mathbb{R}^2_+ \times \mathbb{R} \mapsto \mathbb{R} & \text{such that} \\ \dfrac{1}{c^2}\dfrac{\partial^2 u}{\partial t^2} - \Delta u = \delta(x - x_S) \times \delta(t) & \text{in } \mathbb{R}^2_+, \\ \mathcal{B}^N_{Hig}\, u = 0, & \text{on } \Gamma, \\ u(x,t) = 0, & \text{for } t < 0. \end{cases}$$

is given by:

$$\text{(A.3)} \qquad u(x,t) = G^N_{Hig}(x,t) = G_i(x,t) + G^N_{Hig,r}(x,t),$$

where,

$$\text{(A.4)} \qquad \left| \begin{array}{l} G_i\,(x,t) = \dfrac{1}{2\pi\sqrt{t^2 - \frac{r(x)^2}{c^2}}}\, H(c\,t - r(x)), \\ \\ G^N_{Hig,r}(x,t) = \dfrac{1}{2\pi\sqrt{t^2 - \frac{r^*}{c^2}}} \left[\prod_{j=1}^{n} \rho_j(x,t)\right] \cos\left[\sum_{j=1}^{n} \psi_i(x,t)\right]\, H(c\,t - r^*(x)). \end{array} \right.$$

where $\rho_j(x,t)$ and $\psi_i(x,t)$ are given by

$$\text{(A.5)} \qquad \rho_j(x,t) = \sqrt{\frac{(t\cos\alpha_j - r^*(x)\cos\theta)^2 + r^*(x)^2\sin^2\theta\sin^2\alpha_j}{(t\cos\alpha_j + r^*(x)\cos\theta)^2 + r^*(x)^2\sin^2\theta\sin^2\alpha_j}}$$

$$\text{(A.6)} \qquad \rho_j(x,t) = \sqrt{\frac{(t\cos\alpha_j - (x_2+h))^2 + x_1^2\sin^2\alpha_j}{(t\cos\alpha_j + (x_2+h))^2 + x_1^2\sin^2\alpha_j}}$$

and

$$\psi_j(x,t) = \arccos\left[\frac{r^*(x,t)^2 - \cos^2\alpha_j(r^*(x,t)^2\sin^2\theta - c^2t^2)}{\rho_j(x,t)}\right] \tag{A.7}$$

$$\psi_j(x,t) = \arccos\left[\frac{r^*(x,t)^2 - \cos^2\alpha_j(x_1^2 - c^2t^2)}{\rho_j(x,t)}\right] \tag{A.8}$$

Thanks to (A.5), one can see that the function $x \mapsto G^N_{Hig,r}(x,t)$ is singular on the circle $r^*(x) = ct$ except in the directions α_j.

References

[1] B. Alpert, L. Greengard, and T. Hagström. Rapid evaluation of nonreflecting boundary kernels for the time-domain wave equation. *SIAM J. Numer. Anal.*, 37:1138–1164, 2000.

[2] B. Alpert, L. Greengard, and T. Hagström. Nonreflecting boundary conditions for the time-dependent wave equation. *J. Comput. Phys.*, 180:270–296, 2002.

[3] G.A. Baker. Essentials of padé approximants. Academic Press (New York), 1975.

[4] H. Barucq. A new family of first-order boundary conditions for the Maxwell system: derivation, well-posedness and long-time behavior. *J. Math. Pures Appl.*, 9(1):67–88, 2003.

[5] J. P. Bérenger. A Perfectly Matched Layer for the Absorption of Electromagnetic Waves. *J. of Comp. Phys.*, 114:185–200, 1994.

[6] J.P. Bérenger. Three-dimensional perfectly matched layer for the absorption of electromagnetic waves. *J. of Comp. Phys.*,, 127:363–379, 1996.

[7] L. Cagniard. Réflexion et Réfraction des Ondes Sismiques Progressives. Gauthier-Villard, 1939.

[8] T. Ha Duong and P. Joly. On the stability analysis of boundary conditions for the wave equation by energy methods; Part I : The homogeneous case . *Math. of Comp.*, 62(206):539–563, 1994.

[9] B. Engquist and L. Halpern. Far field boundary conditions for computation over long time. *Appl. Numer. Math.*, 4(1):21–45, 1988.

[10] B. Engquist and L. Halpern. Long-time behaviour of absorbing boundary conditions. *Math. Methods Appl. Sci.*, 13(3):189–203, 1990.

[11] B. Engquist and A. Majda. Absorbing boundary conditions for the numerical simulation of waves. *Math. Comp*, 31:629–651, 1977.

[12] B. Engquist and A. Majda. Radiation boundary conditions for acoustic and elastic wave calculations. *Comm. Pure Appl. Math.*, 32:314–358, 1979.

[13] D. Givoli. Exact and High Order Non-Reflecting Computational Boundaries. In G. Cohen, E. Heikkola, P. Joly, and P. Neittanmaki, editors, *Mathematical and Numerical spects of Wave Propagation*. Springer, 2003.

[14] M. J. Grote and J. B. Keller. Exact nonreflecting boundary conditions for the time dependent wave equation. *SIAM J. Appl. Math.*, 55:280–297, 1995.

[15] M. J. Grote and J. B. Keller. Nonreflecting boundary conditions for time dependent scattering. *J. Comp. Physics*, 127:52–81, 1996.

[16] T. Hagström. On the convergence of local approximations to pseudo-differentials operators. In E. Bécache, G. Cohen, P. Joly, and J. Roberts, editors, *Proceedings of the 3rd Int. Conference on Mathematical and Numerical spects of Wave Propagation Phenomena*. SIAM, 1995.

[17] T. Hagström. Radiation boundary conditions for the numerical simulation of waves. *Acta Numerica*, 8, 1999.

[18] T. Hagström. New results on absorbing layers and radiation boundary conditions. In M. Ainsworth, P. Davies, D. Duncan, P. Martin, and B. Rynne, editors, *Topics in Computational Wave Propagation - Direct and Inverse Problems*, Lecture Notes in Computational Science and Engineering. Springer, 2003.

[19] L. Halpern and J. Rauch. Error analysis for absorbing boundary conditions. *Numer. Math.*, 51:459–467, 1987.

[20] R. L. Higdon. Absorbing boundary conditions for difference approximations to the multi-dimensional wave equation. *Math. Comp.*, 47:437–459, 1986.

[21] R. L. Higdon. Initial-boundary value problems for linear hyperbolic systems. *SIAM Review*, 28(2):177–217, 1986.

[22] R. L. Higdon. Numerical absorbing boundary conditions for the wave equation. *Math. Comp.*, 4:65–90, 1987.

[23] J.H.M.T. Van Der Hijden. Propagation of transient elastic waves in stratified anisotropic media. North Holland Series in Applied Mathematics and Mechanics. Elsevier Science Publishers, 1987.

[24] A. T. De Hoop. The surface line source problem. *Appl. Sci. Res. B*, 8:349–356, 1959.

[25] H. O. Kreiss. Initial boundary value problems for hyperbolic systems. *Comm. Pure Appl. Math.*, 23:277–298, 1970.

[26] L. N. Trefethen and L. Halpern. Well-posedness of one-way wave equations and absorbing boundary conditions. *Math. Comp.*, 47, 1986.

Unité de recherche INRIA Rocquencourt
Domaine de Voluceau - Rocquencourt - BP 105 - 78153 Le Chesnay Cedex (France)

Unité de recherche INRIA Lorraine : LORIA, Technopôle de Nancy-Brabois - Campus scientifique
615, rue du Jardin Botanique - BP 101 - 54602 Villers-lès-Nancy Cedex (France)
Unité de recherche INRIA Rennes : IRISA, Campus universitaire de Beaulieu - 35042 Rennes Cedex (France)
Unité de recherche INRIA Rhône-Alpes : 655, avenue de l'Europe - 38330 Montbonnot-St-Martin (France)
Unité de recherche INRIA Sophia Antipolis : 2004, route des Lucioles - BP 93 - 06902 Sophia Antipolis Cedex (France)

Éditeur
INRIA - Domaine de Voluceau - Rocquencourt, BP 105 - 78153 Le Chesnay Cedex (France)
http://www.inria.fr
ISSN 0249-6399